ELSEVIER

Marine Geology 156 (1999) 5–39

MARINE GEOLOGY
INTERNATIONAL JOURNAL OF MARINE GEOLOGY, GEOCHEMISTRY AND GEOPHYSICS

Response of Western Pacific marginal seas to glacial cycles: paleoceanographic and sedimentological features [1]

Pinxian Wang *

Laboratory of Marine Geology, Tongji University, Shanghai 200092, China

Received 24 June 1997; accepted 6 July 1998

Abstract

This paper reviews the recent progress in late Quaternary studies in five northwestern Pacific marginal seas, especially the South China Sea as an example. A series of marginal seas separate Asia from the Pacific Ocean, and significantly modify the material and energy flux linkage between land and sea. During glacial cycles, the sea-level-induced environmental signal was amplified in the marginal seas, giving rise to drastic changes in areas and configurations of these seas, and to reorganization of sea water circulation in basins. Since most of the Western Pacific marginal seas are influenced by monsoon circulation and some of these are located within the Western Pacific warm pool, the glacial geographic changes have produced a profound impact on regional and global climate. For example, the decrease of sea area and sea surface temperature (SST) in the marginal seas was one of the factors responsible for the enhanced aridity of inland China during the glaciation. Glacial intensification of the winter monsoon and increased seasonality of SST in marginal seas might explain, at least partly, the apparent discrepancy between the tropical paleotemperature estimations based on terrestrial and open-ocean records in this region. As the Western Pacific marginal seas trap terrigenous material supplied by East Asia, the deep-water sedimentation rates there can be one to two orders of magnitude higher than in the open ocean. Down-slope sediment transport is more active when the sea-level changes, particularly during the deglaciation. At least four types of carbonate cycles have been recognized in the Western Pacific marginal seas, and each of those contains environmental signals from the surface and deep sea water, as well as from the drainage basin.

Keywords: marginal seas; Western Pacific warm pool; last glacial maximum; sedimentation rate; carbonate cycles; paleoclimate

1. Introduction

A series of marginal seas ranging from the Bering Sea in the north to the Banda Sea in the south (Fig. 1), separates Asia from the Pacific, the largest continent from the largest ocean, straddling the world's largest subduction zone of the Western Pacific. In the modern global ocean, more than 75% of the marginal basins are concentrated in the Western Pacific continental margin (Tamaki and Honza, 1991). Their formation were closely related to the late Cenozoic deformation of Asia and the subduction of the Pacific plate. Under shearing stress from

* Tel.: +86 21 65983207; Fax: +86 21 65138808; E-mail: pxwang@online.sh.cn

[1] Project supported by the National Natural Science Foundation of China.

PII: S0025-3227(98)00172-8

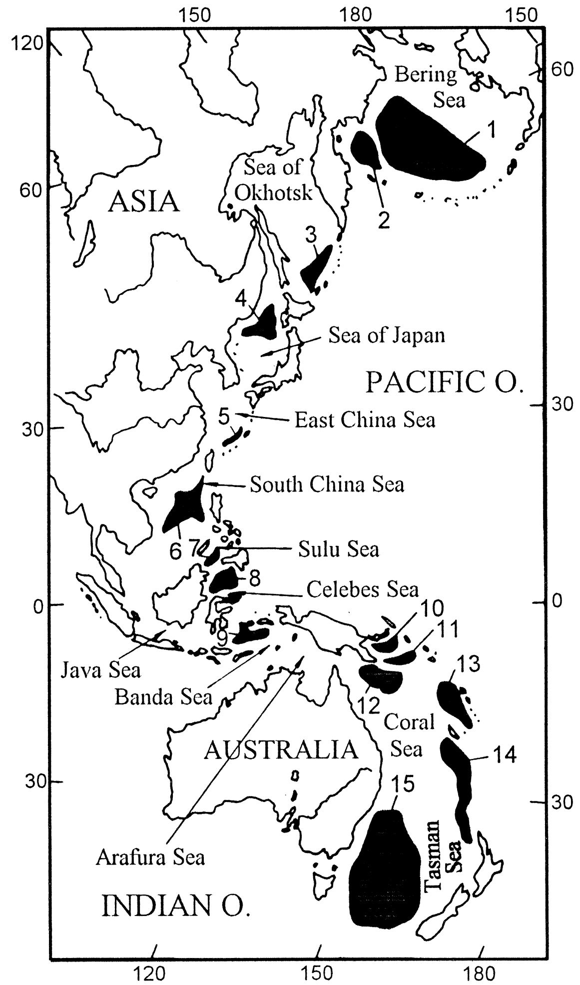

Fig. 1. Western Pacific marginal seas with marginal basins (black areas). Marginal basins without clear geographic expression (e.g., Philippine Basin, Mariana Basin, Lau Basin, Fiji Basins) are not shown. Marginal basins: *1* = Aleutian Basin; *2* = Komandosky Basin; *3* = Kuril Basin; *4* = Japan Basin; *5* = Okinawa Trough; *6* = South China Basin; *7* = Sulu Basin; *8* = Celebes Basin; *9* = Banda Basin; *10* = Soloman Basin; *11* = Woodlark Basin; *12* = Coral Basin; *13* = N. Loyalty Basin; *14* = New Caledonia Basin; *15* = Tasman Basin.

the India–Asia collision and extensional stress from the Pacific subduction, Asia has become the highest continent, together with numerous marginal basins along its margin (Jolivet et al., 1989, 1994). Since their formation in the late Cenozoic, the marginal seas have become a unique tectonic and geographic feature in the Western Pacific region and as such must have a profound climatic and environmental impact on the region. This impact has been most prominent during the late Quaternary glacial cycles when the eustatic sea-level fluctuations resulted in major landward and seaward migrations of the coastline, and the closure and opening of the seaways between the marginal seas and the ocean led to reorganization of the sea water circulation (P. Wang, 1996).

Ocean Drilling Program activities from 1988 to 1991 have brought fundamental changes to our understanding of volcanism, crustal deformation and sedimentation in the Western Pacific marginal basins, particularly in the Sea of Japan and Sulu Sea (Taylor and Natland, 1995). On the other hand, late Quaternary paleoceanography and sedimentology in the Western Pacific marginal seas progressed greatly thanks to a number of successful expeditions in the last years, especially to the South China Sea and the Okinawa Trough areas. As well known, the material and energy flux between land and sea is of primary importance for the global climatic change at various time scales, and this linkage of flux is complicated by the occurrence of marginal seas, but their role in the global climate change has yet to be recognized. The present paper is an attempt at reviewing the recent progress in late Quaternary studies of the Western Pacific marginal seas, in order to show the regional and global climatic significance of marginal seas in the glacial cycles.

2. Morphology and types of marginal seas

2.1. Morphological types

A great variety of marginal seas exist in the modern world. According to the location in different climatic zones, Seibold (1970) distinguished two types of marginal seas: the humid and arid types with estuarine and anti-estuarine circulation of water, represented by the Baltic Sea and the Persian Gulf, respectively (Seibold and Berger, 1993, pp. 203–207). All modern marginal seas of the Western Pacific are located in the humid zone, where the marginal seas are different in terms of their extent of connection with the open ocean, largely depending on their morphological features. In an attempt to quantify the difference, we used the ratio of sill

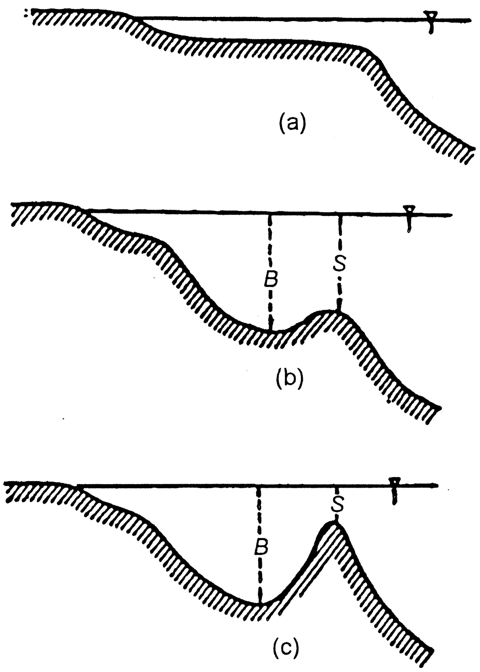

Fig. 2. Schematic profiles of three types of marginal seas: (a) shallow bank type; (b) open basin type; (c) enclosed basin type. B = basin depth; S = sill depth. (After P. Wang et al., 1997.)

depth (S) to basin depth (B) and the proportion of shallow water part to distinguish three types of marginal seas in the Western Pacific: (1) shallow-bank type (Fig. 2a); (2) open-basin type (Fig. 2b); and (3) enclosed-basin type (Fig. 2c). The first type includes the Yellow Sea with the Bohai Gulf and the Arafura Sea with the Gulf of Carpentaria, but these are not marginal seas in the tectonic sense but shelf extensions of marginal seas. The open-basin type is represented by the East China Sea and the Sea of Okhotsk where the sill depth is more or less close to the basin depth ($S/B > 0.5$), while the enclosed-basin type includes basins such as the Sea of Japan, South China Sea, and Sulu Sea with a sill depth much shallower than the basin depth ($S/B < 0.5$; P. Wang, 1991; P. Wang et al., 1997).

However, the S/B ratio describes the basin morphology only in vertical profile, whereas the extent of isolation in plan view or in three-dimensional view should also be considered. Thus, we propose to use two more ratios: the ratio of the passage width (P) to the total surface area (A) of the sea (Fig. 3), and the ratio of the area of connecting section (C) to the total volume of the basin (V) (Fig. 4). Here the 'passage width' is the sum of linear distances between both sides for each of the passages of a given basin; the 'connecting section' denotes a vertical section of the open part of the basin connecting with the ocean or other seas. A combination of the three ratios (S/B, P/A, C/V) may provide a comparatively full description of the extent of isolation of a marginal sea. The smaller the sum of ratios, the more isolated is the basin. Nine marginal seas between the Western Pacific and Asia are compared and ranked as follows (Table 1).

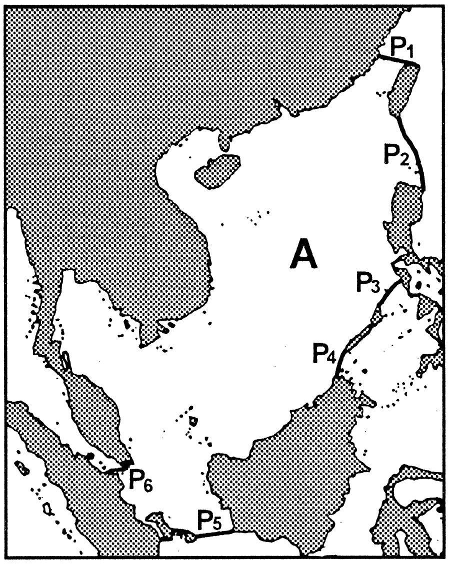

Fig. 3. Diagram showing the measurement of morphological feature of a marginal sea in plain, on example of the South China Sea: A = surface area; P = passage length ($P = P_1 + P_2 + P_3 + P_4 + P_5 + P_6$).

2.2. Enclosed-basin type

As seen from Table 1, the Sea of Japan is distinguished by the highest extent of isolation, followed by the South China Sea, Sulu Sea, and Sea of Okhotsk. These seas with lower ratios in Table 1 can be considered as basins of the enclosed type, while the Celebes Sea, Banda Sea, East China Sea and Java Sea belong to the open-basin type. Although the differentiation of both basin types is quite arbitrary, the two groups of marginal seas in the western Pacific responded differently to the glacial cycles. The seas

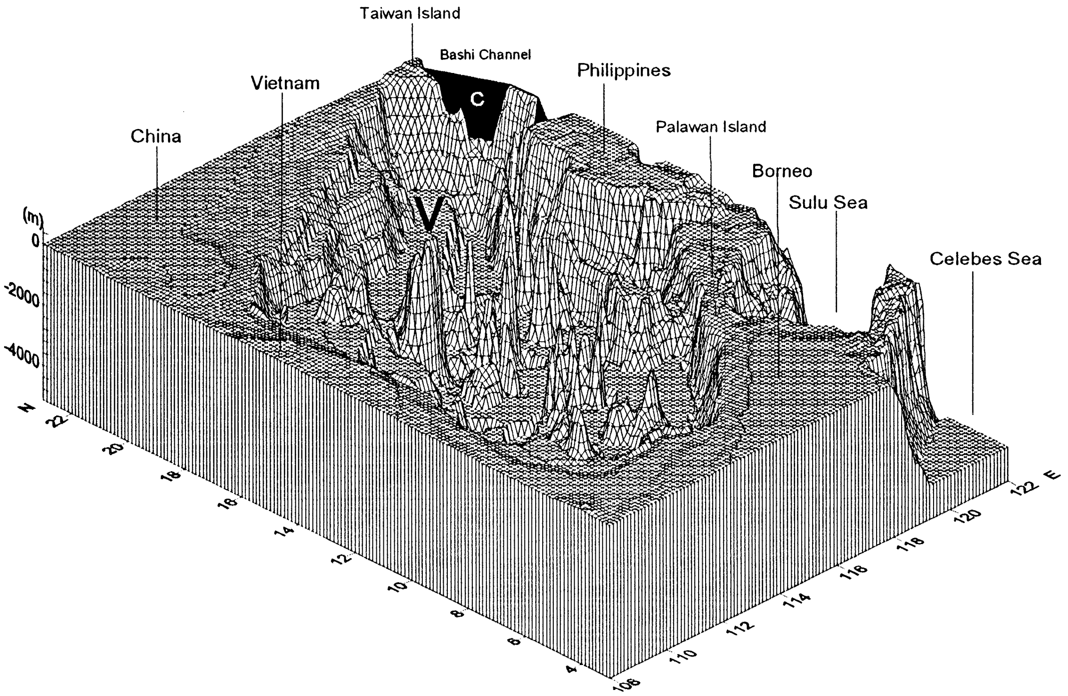

Fig. 4. Diagram showing the measurement of three-dimensional features of a marginal sea, with the South China Sea as example: V = basin volume; C = area of connecting section (in black). Only the Bashi Strait is shown, all the other passages are too shallow to be visible in the diagram).

of the enclosed-basin type have been much more sensitive to the glacial sea-level lowering.

The paleoceanographic interest of the marginal seas of the enclosed-basin type lies in the temporal changes of their connection with the ocean, and of the interconnection of marginal basins through passages of various sizes. The closure of seaways through the Indonesian Archipelago during the Last

Table 1
Morphological features of the Western Pacific marginal seas

Marginal sea	Average depth (m)	Shallow sea area (<200 m; %)	Basin depth, B (m)	Sill depth, S (m)	S/B	Passage width, P (km)	Surface area, A (10^3 km^2)	P/A	Connecting section, C (km^2)	Basin volume, V (10^5 km^3)	C/V (10^{-5})
Enclosed-basin type											
Sea of Japan	1361	26.3	4049	130	0.03	136	978	0.14	8	1713	0.48
South China Sea	1212	52.4	5377	2600	0.48	950	3500	0.27	493	4242	11.61
Sulu Sea	1570	34.3	5580	420	0.08	527	348	1.52	88	553	15.91
Sea of Okhotsk	777	41.2	3374	~2000	0.59	455	1590	0.29	184	1365	13.48
Open-basin type											
Celebes Sea	3364	10.8	6200	1400	0.23	647	435	1.49	453	1586	28.58
Banda Sea	2737	8.3	7440	3130	0.42	1092	695	1.57	730	2129	34.31
East China Sea	370	75.6	2719	>2000	0.74	981	1228	0.80	321	303	105.96
Java Sea	46	90.4	1720	1720	1	1175	480	2.45	416	22	1889.5

Data of morphological features from: Fairbridge, 1966; Gorshkov, 1974; Torgersen et al., 1983. Due to the miscellaneous data sources the figures in the table may not be consistent in terms of sea area, etc.

Table 2
Straits of the Japan Sea and the South China Sea

Marginal sea	Strait	Connected sea	Sill depth	Minimal width (km)
Sea of Japan	Tartar	Okhotsk	8 m ?	7
	Soya	Okhotsk	44 m	42
	Tsugaru	Pacific	116 m	19
	Korean	East China	131 m	116
South China Sea	Taiwan	East China	70 m	130
	Bashi	Pacific	2.2 km	370
	Mindoro	Sulu	420 m	125

Glacial Maximum (LGM), for example, led to a cessation of the Leeuwin Current and hence a decrease of sea surface temperature along the western coast of Australia (Wells and Wells, 1994). The Sulu Sea is completely surrounded by a shallow shelf, and its deep-water exchange is restricted to the Mindoro Strait with a sill depth of 420 m (Table 2, Fig. 1). Surface and intermediate water of the South China Sea spills over the sill and enters the Sulu Sea, giving rise to a remarkably homogeneous deep water there with a nearly uniform temperature (9.8º–10.0ºC) and salinity (34.5‰) (Linsley and Dunbar, 1994). Because of the present shallow sill depth of the Mindoro Strait, the 5000-m-deep basin has an unusually high deep-water temperature near 10ºC, but the greater sill depth about 2.4 million years ago allowed cooler water to enter the Sulu Sea and led to increased carbonate dissolution (Linsley, 1991).

Even more isolated is the Sea of Japan, which is distinguished from all the other marginal seas in the West Pacific by its extremely shallow sills. During the LGM only two of the four connecting straits of the basin were deep enough to maintain water exchange with the Pacific (Tsugaru Strait, sill depth 116 m) and with the East China Sea (Tsushima Strait, sill depth 131 m; Table 2). As the sill depths are very close to that of the LGM sea-level lowstand, the Sea of Japan was almost isolated from the ocean. At the present time, the Tsushima Current, a branch of Kuroshio Current, carries warm and saline water from the East China Sea into the Sea of Japan through the Korean (or Tsushima) Strait (about 97% of water input into the sea; Gorbarenko, 1993). Then this water flows northward and leaves the Japan Sea mainly through the Tsugaru Strait (Chen et al., 1995) into the Pacific mixing with the Oyashio cold water. Because of the enclosed nature of the basin, the deep water of the Japan Sea has no direct exchange with the Pacific or other marginal seas. Below 200–300 m, the Sea of Japan is occupied by the very homogeneous Japan Sea Proper Water (Sudo, 1986) which is generated in the northern half of the basin in winter at conditions of low temperature and high wind stress (Chen et al., 1995). Because of its formation inside the basin and the frequent turnover, the deep water in the Sea of Japan is distinguished by its vertical homogeneity (salinity being consistently 34.07 ± 0.005‰), unusually high oxygen content and young age (about 120 years, Chen et al., 1995).

Among marginal seas of the enclosed-basin type, the Okhotsk Sea ranks the last in terms of the extent of isolation, with the three ratios (S/B, P/A, C/V) slightly exceeding those of the South China Sea (Table 1). However, oceanography of the Okhotsk Sea had been poorly known until the very recent studies showing that “water properties in the Okhotsk Sea are very different from those of the North Pacific” (Talley and Nagata, 1995). The passages of the Okhtsk Sea to the Pacific are the straits between the Kuril Islands, and its circulation is connected in a complex way with the cyclonic circulation of the subarctic North Pacific. The North Pacific water flows into the Okhotsk Sea primarily through straits in the northern part of the Kuril Islands area and flows out of the Okhotsk Sea mostly through straits in the southern part. As shown by a Russian cruise in 1991, the water properties on the two sides of the Kuril Islands differ from each other significantly, indicating the barrier role of the islands (Gladyshev, 1993). Thus, the dichothermal layer (temperature minimum) in the Okhotsk Sea is colder and the mesothermal layer (temperature maximum) is much deeper (at about 1000 m) than in the Northern Pacific Ocean (at about 250 m). The Okhotsk Sea also contains the North Pacific’s freshest, most oxygenated water at densities greater than 27.2 sigma-theta (Talley, 1996). Of interest is the Soya Current entering the Okhotsk Sea through Soya Strait from the Japan Sea and originating from the Tsushima Current. Within the Okhotsk Sea, the incoming North Pacific water properties are changed under the important influence of the relatively warm and saline Soya Current water, the fresh Amur river discharge and the sea ice production (P. Wang, 1998).

As shown below, all these inter-basinal connections make their notable impact on sedimentological and paleoceanographic features of the basins.

3. Sedimentological response

3.1. Sedimentation rates

Unlike the Atlantic and Indian Oceans, there is no large submarine deep-sea fan formed in the Western Pacific. Southern and Eastern Asia with their islands provide >70% of the terrigenous suspended material supplied to the global ocean (Milliman and Meade, 1983). Marginal seas intercept sediments and prevent the accumulation of deep-sea fans in the Pacific Ocean. Hence, the deep-water sedimentation rates in the marginal seas can be one to two orders of magnitude higher than in the open ocean. Fig. 5 show the variations of Holocene sedimentation rates in the marginal seas and the western Pacific based on data from 100 cores (see Table 3 for locations of the cores and sources of the data). The Holocene sedimentation rate fluctuates around 2 cm/ka in the Pacific, whereas it may exceed 50 cm/ka in the marginal seas. In the East China Sea, the Holocene sedimentation rate ranges from 2.33 to 36.66 cm/ka, averaging 10.7 cm/ka; in the South China Sea it varies from 1.67 to 66.67 cm/ka, averaging 8.0 cm/ka; in the Sea of Japan, the rate ranges from 2.92 to 22.50 cm/ka, with an average of 10.5 cm/ka.

However, the Holocene sedimentation rates in Table 3 are mostly calculated from the thickness of Holocene deposits based on oxygen-isotopic and/or biostratigraphic analysis without C-14 datings. As known, “Holocene sediments in the sea are mostly water” and in most cases there is a question of the completeness of the record recovered, due to blowing away of surficial sediment by the falling coring device (Hay, 1994). Therefore, the sedimentation rates are useful in their comparison, and the higher values in a given basin are more informative than the lower ones. As seen from Fig. 5, the marginal seas from lower latitudes have higher sedimentation rates than those from higher latitudes. Moreover, in basins with sufficient water depths, such as the Sea of Japan and the South China Sea, the maximal rates appear at the depth interval of 2000–2500 m, below the upper slope where sediments move down-slope and above the lysocline where carbonates start to dissolve intensively. In the Sulu Sea, the occurrence of the maximum rate of 50 cm/ka below CCD at 4500 m results from frequent turbidites (see below). The high sedimentation rates in the East China Sea (Okinawa Trough) are related to the contribution of terrigenous material by large rives such as Changjiang (Yangtze River) and Huanghe (Yellow River). Thus, the sedimentation rates vary between basins and within the basin.

In contrast to the open ocean (such as the Ontong-Java Plateau, Berger et al., 1993), the temporal variations of sedimentation rates in the marginal seas are large. This can be demonstrated with the South China Sea as an example, where the glacial sedimentation rate is twice as high as during postglacial times (P. Wang et al., 1995). Using sediment thickness data of 73 cores, ranging from 220 m to 4300 m in water depth, Huang and Wang (1998) show the average accumulation rates for six areas in the SCS (Fig. 6; Table 4). The accumulation rate averages 4.92 g cm^{-2} ka^{-1} for the oxygen isotope stage 1 or Holocene, and 8.95 g cm^{-2} ka^{-1} for stage 2 or last glacial. For the oxygen isotope stage 1 the maximum rates occur in the northeastern part (13.3 g cm^{-2} ka^{-1}) off the Pearl River mouth, but for stage 2 the maximal values moved to the southwestern part (17.9 g cm^{-2} ka^{-1}) where the Paleo-Sunda River entered the sea (C. Wang and Chen, 1990). Therefore, the accumulation rates depend very much on the sediment discharge from rivers. During the glacial time the erosion of the newly exposed shelf and the direct discharge of terrigenous fluvial matter into the deep sea increased the glacial accumulation rates. The Paleo-Sunda River that drained large areas of Indonesian mountainous islands was responsible

Fig. 5. Sedimentation rates for the Holocene (oxygen isotope stage 1) in the Western Pacific and its marginal seas (see Table 3 for data sources; horizontal axis = water depth).

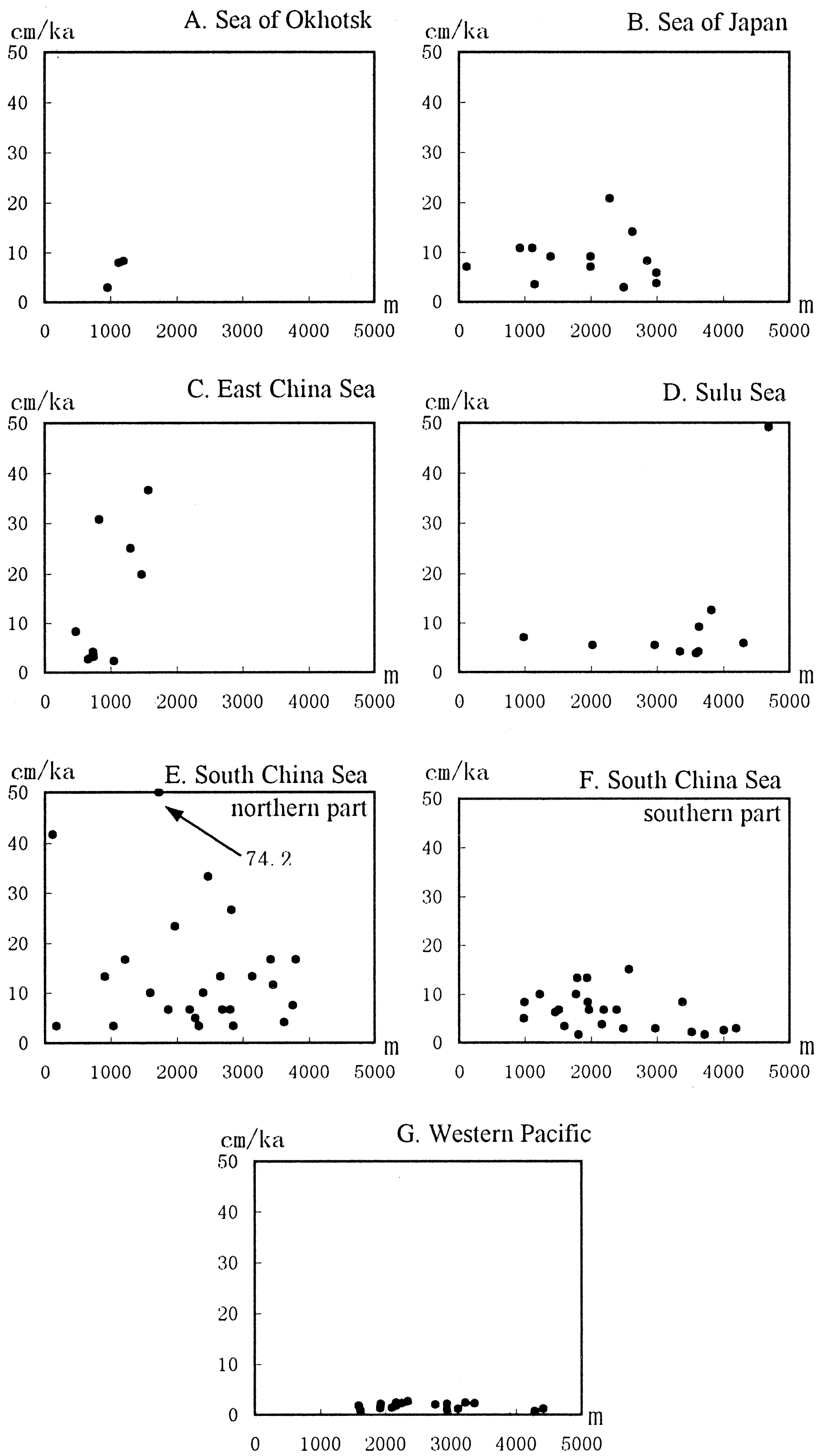
A. Sea of Okhotsk
B. Sea of Japan
C. East China Sea
D. Sulu Sea
E. South China Sea
northern part
74.2
F. South China Sea
southern part
G. Western Pacific
cm/ka
m
0 10 20 30 40 50
0 1000 2000 3000 4000 5000

Table 3
Holocene Sedimentation rates in Western Pacific and its marginal seas (used in Fig. 5)

Sea	Site	Site location	Water depth (m)	Sedimentation rate (cm/ka)	Reference
Okhotsk Sea	Volkanolog 34-91	49ºN, 150ºE	1200	8.33	Keigwin, 1994; Gorbarenko, 1991b
	K-105	52º53′N, 150º24′E	1130	7.92	Gorbarenko, 1991a,b
	K-68	49º55′N, 149º37′E	960	3.75	Ibid.
Japan Sea	ODP 797	38º37′N, 134º32′E	2862	9.17	Tada et al., 1992
	GH93-KI-4	39º46′N, 138º46′E	2293	20.83	Ikehara et al., 1994
	GH92-703	39º30′N, 136º30′E	2638	14.17	Ibid.
	J-3RGA	35º54′N, 130º15′E	1400	9.17	Gorbarenko et al., 1995
	J-11RGA	40º07′N, 133º59′E	1150	3.58	Ibid.
	KH-77-3, M-2	36º26′N, 134º10′E	1115	10.83	Oba, 1982
	KH-79-3,C-3	37º04′N, 134º42′E	935	10.83	Ibid.
	76104	35º19′N, 131º07′E	125	7.08	Gorbarenko, 1993
	1682	41º51′N, 132º24′E	~3000	5.83	Gorbarenko, 1987
	2153	49º12′N, 133º41′E	~3000	3.75	Ibid.
	1681	41º52′N, 132º24′E	2500 ~ 3000	2.92	Ibid.
	1670	39º55′N, 133º30′E	2000	7.08	Gorbarenko, 1993
	1639	38º40′N, 137º13′E	2000	9.17	Gorbarenko, 1991b
East China Sea	255	25º12′N, 123º06′E	1575	36.66	Jian et al., 1996
	170	26º38′N, 125º48′E	1470	19.83	Ibid.
	C2-5	26º10′N, 126º25′E	1300	25.00	Cang and Yan, 1992
	RN80-PC3	29º04′N, 127º23′E	830	30.83	Xu and Oda, 1995
	Z14-6	27º07′N, 127º27′E	739	4.17	Cang and Yan, 1992
	Z1-4	31º17′N, 128º34′E	472	8.33	Ibid.
	1595	32º06′N, 129º16′E	660	2.67	Gorbarenko, 1993
	7008	24º23′N, 122º57′E	745	3.17	Gorbarenko, 1991b
	7045	25º23′N, 123º13′E	1050	2.33	Ibid.
South China Sea north part	ZQ4	21º00′N, 115º25′E	124	41.67	Min et al., 1992
	N204	18º13′N, 110º56′E	180	3.33	Gao et al., 1992
	17943	18º57′N, 117º33′E	917	13.33	Sarnthein et al., 1994
	SO 49-8KL	19º11′N, 114º12′E	1040	3.33	Wang and Wang, 1990; Schönfeld and Kudrass, 1993
	17944	18º40′N, 113º38′E	1219	16.67	Sarnthein et al., 1994
	V36-6	19º47′N, 115º49′E	1597	10.00	Feng et al., 1988
	17940	20º07′N, 117º23′E	1728	66.67	Sarnthein et al., 1994
	17950	16º06′N, 112º54′E	1868	6.67	Ibid.
	17933	19º32′N, 116º14′E	1972	23.33	Ibid.
	17949	17º21′N, 115º10′E	2195	6.67	Ibid.
	17952	16º40′N, 114º28′E	2282	5.00	Ibid.
	17951	16º17′N, 113º25′E	2340	3.33	Ibid.
	17945	18º08′N, 113º47′E	2404	10.00	Ibid.
	17939	19º59′N, 117º27′E	2473	33.33	Ibid.
	17934	19º02′N, 116º28′E	2665	13.33	Ibid.
	SO50-37KL	18º55′N, 115º46′E	2695	6.67	Winn et al., 1992; Schönfeld and Kudrass, 1993
	V36-3	19º01′N, 116º06′E	2809	6.67	Wang and Wang, 1990
	17938	19º47′N, 117º32′E	2835	26.67	Sarnthein et al., 1994
	17948	16º43′N, 114º54′E	2855	3.33	Ibid.
	17935	18º53′N, 116º32′E	3143	13.33	Ibid.
	17937	19º30′N, 117º40′E	3428	16.67	Ibid.
	17946	18º08′N, 114º15′E	3465	11.67	Ibid.

Table 3 (continued)

Sea	Site	Site location	Water depth (m)	Sedimentation rate (cm/ka)	Reference
	SO49-14KL	18º18′N, 114º14′E	3634	4.17	Jin et al., 1989
	SO50-29KL	18º20′N, 115º59′E	3766	7.50	Winn et al., 1992; Schönfeld and Kudrass, 1993
	17936	18º46′N, 117º07′E	3809	16.67	Sarnthein et al., 1994
South China Sea south part	GGC13	10º36′N, 118º17′E	990	5.00	Miao et al., 1994
	8757		1000	8.33	
	17963	6º10′N, 112º40′E	1233	10.00	Sarnthein et al., 1994
	GGC9	11º38′N, 118º38′E	1465	6.25	Miao et al., 1994
	17954	14º46′N, 111º32′E	1517	6.67	Sarnthein et al., 1994
	GGC10	11º43′N, 118º31′E	1605	3.33	Thunell et al., 1992; Miao et al., 1994
	8350	9º20′N, 109º48′E	1780	10.00	Astakhov et al., 1989
	17961	8º30′N, 112º20′E	1795	13.33	Sarnthein et al., 1994
	SCS15A	10º24′N, 114º14′E	1812	1.67	C. Wang et al., 1986
	RC12-350	6º33′N, 111º13′E	1950	13.33	Jian, 1992
	17959	11º08′N, 115º17′E	1957	8.33	Sarnthein et al., 1994
	17962	7º11′N, 112º05′E	1970	6.67	Ibid.
	GGC11	11º53′N, 118º20′E	2165	3.75	Thunell et al., 1992; Miao et al., 1994
	17957	10º51′N, 115º18′E	2197	6.67	Sarnthein et al., 1994
	17955	14º07′N, 112º11′E	2393	6.67	Ibid.
	GGC12	11º56′N, 118º13′E	2495	2.92	Thunell et al., 1992; Miao et al., 1994
	17958	11º37′N, 115º05′E	2581	15.00	Sarnthein et al., 1994
	GGC6	12º09′N, 118º04′E	2975	2.92	Thunell et al., 1992; Miao et al., 1994
	17956	13º51′N, 112º35′E	3387	8.33	Sarnthein et al., 1994
	GGC4	12º39′N, 117º56′E	3530	2.08	Thunell et al., 1992; Miao et al., 1994
	GGC3	13º16′N, 117º48′E	3725	1.67	Ibid.
	GGC2	13º37′N, 117º41′E	4010	2.50	Ibid.
	GGC1	14º00′N, 117º30′E	4203	2.92	Ibid.
Sulu Sea	SO58-69KL	8º50′N, 121º36′E	4696	49.17	Quadfasel et al., 1990
	ODP769	8º47′N, 121º13′E	3643	9.17	Linsley and Thunell, 1990
	GGC41	7º13′N, 119º32′E	3590	3.75	Miao et al., 1994
	GGC34	6º54′N, 119º10′E	2970	5.42	Ibid.
	GGC27	8º30′N, 118º15′E	2030	5.42	Ibid.
	GGC23	8º09′N, 118º34′E	990	7.08	Ibid.
	SO49-96KL	8º11′N, 119º28′E	3634	4.17	Vollbrecht and Kudrass, 1990
	SO58-67KL	8º50′N, 121º20′E	3350	4.17	Ibid.
	SO58-80KL	8º02′N, 121º14′E	4313	5.83	Ibid.
	SO58-82KL	8º04′N, 121º52′E	3824	12.5	Ibid.
West Pacific	ERDC125BX	0º00′S, 161º00′E	3368	2.33	Berger et al., 1987
	ERDC124P	0º01′S, 160º24′E	2948	1.08	Ibid.
	ERDC123BX	0º01′S, 160º25′E	2946	2.17	Ibid.
	ERDC79BX	2º47′N, 156º14′E	2766	2.00	Ibid.
	ERDC83BX	1º24′N, 157º19′E	2342	2.67	Ibid.
	ERDC120BX	0º01′S, 158º42′E	2247	2.25	Ibid.
	ERDC112BX	1º38′S, 159º14′E	2168	2.37	Ibid.
	ERDC113P	1º38′S, 159º13′E	2163	1.75	Ibid.
	ERDC101P	3º15′S, 159º23′E	2106	1.50	Ibid.

Table 3 (continued)

Sea	Site	Site location	Water depth (m)	Sedimentation rate (cm/ka)	Reference
	ERDC88BX	0º03′S, 155º52′E	1923	1.37	Ibid.
	ERDC92 BX	2º14′S, 157º00′E	1598	1.83	Ibid.
	ERDC93P	2º14′S, 157º00′E	1619	0.79	Ibid.
	ERDC89PG	0º00′S, 155º52′E	1932	2.13	Ibid.
	V18-299	16º07′S, 149º40′E	4284	0.6–0.8	Lao et al., 1992
	RC11-210	01º49′N, 140º03′E	4420	1.2	Ibid.
	TT154-10	10º17′S, 111º20′E	3225	2.4	Ibid.
	V19-55	17º00′S, 114º11′E	2177	1.2	Ibid.

for the high sediment supply during the glacial, with its disappearance during the deglaciation leading to a decrease of accumulation rates in the southwestern part of the sea, namely the slope off the Sunda Shelf.

In general, the sedimentation rate within a marginal sea is highest near the river mouths and decreases with distance from the coast. Such a pattern has been recorded in the Sea of Okhotsk (Lisitzin, 1972, fig. 68) and many other basins; both the down-slope and inter-basinal sediment transport can significantly modify this general pattern and lead to enhanced deposition in the abyssal plain or deep-water trench area, as observed in the Sulu Sea and the South China Sea (see discussions below).

3.2. Terrigenous sedimentation and down-slope transport

The Western Pacific marginal seas are covered by biogenic, volcanogenic and especially terrigenous sediments. As the fluvial contribution predominates in the terrigenous component, the highest sedimentation rates occur in the basins where rivers with the largest sediment discharge are emptying. Table 5 shows the major rivers discharging into the five marginal seas discussed in this paper. As can be clearly seen, the East China Sea (with the Bohai Gulf and the Yellow Sea) and the South China Sea are supplied by the largest rivers in the Western Pacific such as the Huanghe (Yellow River), Changjiang (Yangtze River) and Mekong River. The resulting high sedimentation rates are responsible for the occurrences of the globally widest continental shelves. Moreover, the small mountainous rivers draining tectonically active islands in Southeast Asia are also important suppliers of terrigenous material to the sea (Milliman and Syvitski, 1994; see Table 5), having contributed significantly to the building up of the Sunda Shelf.

Nevertheless, the relationship between river discharge and deep-sea deposition is not always simple and straightforward. The highest sedimentation rate of terrigenous clasts does not necessarily occur near the river mouth because of various ways of sediment transport. For example, the accumulation rates of the northeastern slope of the South China Sea are remarkably higher than those in the northwestern slope, west of the Pearl River mouth, although the sediment discharge by the Pearl River is transported westwards due to the Coriolis force, and there is no large river east of the mouth. The sediment supply leading to the unusually high sedimentation rates on the northern slope (e.g., cores 17940, 20º07′N, 117º23′E, water depth 1728 m, with the Holocene thickness of 6.5 m, L. Wang et al., 1999) presumably comes from the East China Sea and the Pacific via the Bashi Strait. As shown by the shallow sedimentary trap (18º28′N, 116º01′E, water depth 3750 m) set up at 1000 m depth in the northeastern South China Sea, the sediment supply is subject to strong seasonal variations, with the maximal flux in winter, from November to February (Jennerjahn et al., 1992), when the winter monsoon drives water currents bringing terrigenous material from the East China Sea or from the eastern coast of Taiwan down to the South China Sea via the Bashi Strait. This is an example of inter-basinal sediment transport which, of course, should not be confined only to the SCS. Another example is the northeastern transport of sediment from the East China Sea to the Sea of Japan by the Tsushima Current through the

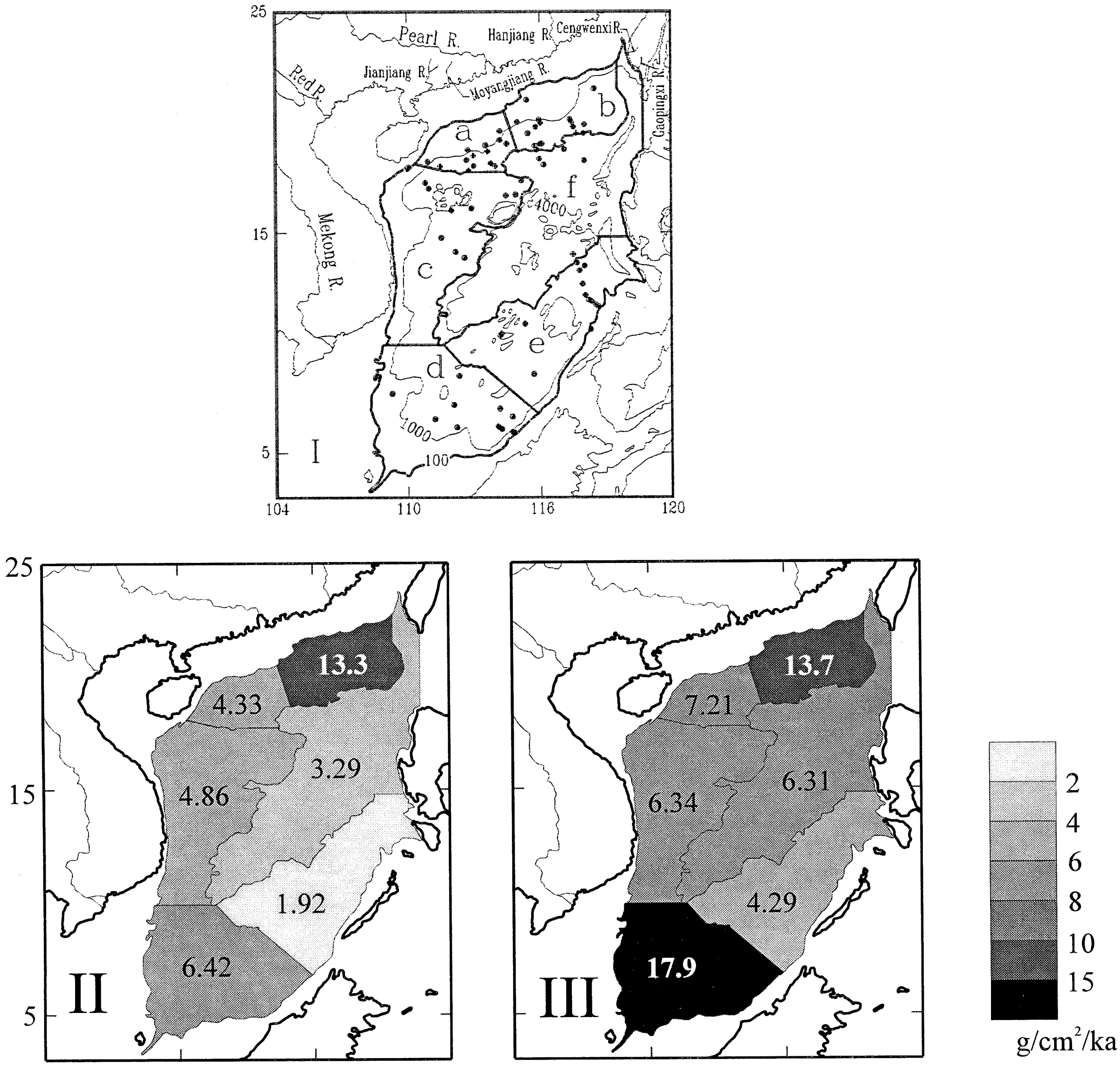

Fig. 6. Average accumulation rates for the Holocene and last glacial (stage 2) in six areas of the South China Sea (g cm^{-2} ka^{-1}) (see Table 4 for data sources) (Huang and Wang, 1998). (I) Sketch map of six areas with core locations; (II) Holocene ($\delta^{18}O$ stage 1); (III) last glacial ($\delta^{18}O$ stage 2).

Tsushima Strait between Japan and Korea (Ikehara, 1992).

A very important complicating factor of the distribution of terrigenous sediment in the marginal seas is its down-slope transport. As seen from Fig. 5, the depositional rates in the marginal seas below the lysocline are by one order of magnitude higher than those in the open ocean, showing the role of sediment capture in marginal seas. In the modern ocean, fluvially discharged particles commonly accumulate in the mid-shelf region, not reaching the deep-water part of the sea (Nittrouer and Wright, 1994). At a geological scale, however, the deposition on continental shelves is usually episodic and will eventually be eroded and transported downslope to the deeper part of the basin. The down-slope transport of sedi-

Table 4
Average accumulation rates for oxygen isotope stages 1 and 2 in the South China Sea (used in Fig. 6) (after Huang, 1997)

Core site	Latitude N	Longitude E	Water depth (m)	Accumul. rate (g cm^{-2} ka^{-1})		Reference
				$\delta^{18}O$ st.1	$\delta^{18}O$ st.2	
17941-2	21.517	118.483	2201	5.52	5.10	Sarnthein et al., 1994
ZQ4	21	115.417	124	29.46	25.08	Min et al., 1992
17940-2	20.117	117.383	1729	37.65	21.45	Sarnthein et al., 1994
17931-2	20.1	115.967	1005	2.05	1.42	Ibid.
G77	20	114.983	895	10.02	3.58	Li, 1993
17939-2	19.983	117.45	2473	19.83	45.21	Sarnthein et al., 1994
17932-2	19.95	116.033	1365	18.67	10.72	Ibid.
RC26-16	19.883	118.033	2912	7.80		Li, 1995
17938-2	19.783	117.533	2835	11.17	33.20	Sarnthein et al., 1994
V36-6	19.783	115.817	1597	7.57	9.29	Feng et al., 1988
SO49-3SL	19.583	114.2	713	3.49		Schönfeld and Kudrass, 1993
17937-2	19.5	117.667	3482	7.25	27.12	Sarnthein et al., 1994
8315	19.5	118.001	3427	7.59		Li, 1993
G76	19.484	115.469	2400	8.84	3.58	Mao and Harland, 1993
SO49-8KL	19.183	114.2	1040	2.28	4.57	Schönfeld and Kudrass, 1993
SO49-12KL	19.017	114.5	1532	1.31	2.99	Schönfeld and Kudrass, 1993
V36-3	19.017	116.1	2809	5.02	10.18	P. Wang et al., 1986; Feng et al., 1988
G73	19	115.986	2970	5.01	4.70	Li, 1993
17943-2	18.95	113.55	917	8.96	23.46	Sarnthein et al., 1994
SO50-37KL	18.917	115.767	2695	6.81	9.29	Schönfeld and Kudrass, 1993
17936-2	18.767	117.117	3809	6.29	22.60	Sarnthein et al., 1994
31KL	18.75	115.867	3360	5.17	7.78	Huang et al., 1997a
G64	18.735	112.751	600	2.36	2.69	Li, 1993
17944-2	18.667	113.633	1219	7.83	10.20	Sarnthein et al., 1994
G65	18.486	113	1659	6.19	6.27	Li, 1993
SO50-29KL	18.333	115.983	3766	4.56	8.83	Schönfeld and Kudrass, 1993
SO49-41KL	18.283	112.683	2120	2.33	2.87	Jin et al., 1989; Mao and Harland, 1993
8328	18.25	118.017	3860	5.14	9.54	Li, 1993
N204	18.217	110.933	180	2.24	4.39	Gao et al., 1992
17945-2	18.133	113.783	2404	6.22	14.19	Sarnthein et al., 1994
V36-1	18.067	116.183	3824	4.72	6.53	Feng et al., 1988
8323	18.017	113.002	2050	5.30	5.37	Li, 1993
8324	18	113.985	3242	7.07	4.93	Ibid.
SCS90-36	18	111.5	2050	3.44	1.84	Huang et al., 1997b
SO49-37KL	17.817	112.783	2004	4.36	7.41	Schönfeld and Kudrass, 1993
17949-2	17.35	115.167	2195	4.07	4.86	Sarnthein et al., 1994
G45	17.251	110.818	1600	8.25	6.72	Li, 1993
G46	16.985	110.984	1310	9.13		Ibid.
17948-2	16.717	114.9	2855	3.49	5.09	Sarnthein et al., 1994
17952-3	16.667	114.467	2882	3.49	10.05	Ibid.
17950-2	16.1	112.9	1868	4.98	8.20	Ibid.
G38	16	112	1115	5.30	6.27	Li, 1993
17954-2	14.767	111.533	1517	4.48	6.81	Sarnthein et al., 1994
17955-2	14.117	112.183	2393	3.98	6.05	Ibid.
GGC-1	14	117.5	4203	2.06	1.82	Miao et al., 1994
17956-2	13.85	112.583	3387	4.07	3.32	Sarnthein et al., 1994
GGC-2	13.617	117.683	4010	1.77	1.80	Miao et al., 1994
8357	13.483	118.017	3949	2.36	5.15	Li, 1993
GGC-3	13.267	117.8	3725	1.20	1.82	Miao et al., 1994

Table 4 (continued)

Core site	Latitude N	Longitude E	Water depth (m)	Accumul. rate (g cm^{-2} ka^{-1})		Reference
				δ^{18}O st.1	δ^{18}O st.2	
GGC-4	12.65	117.933	3530	1.46	3.13	Ibid.
GGC-6	12.15	118.067	2975	2.06	2.47	Ibid.
GGC-12	11.933	118.217	2495	1.99	2.27	Ibid.
GGC-11	11.883	118.333	2165	2.66	3.13	Ibid.
GGC-10	11.717	118.517	1605	2.36	4.01	Ibid.
GGC-9	11.633	118.633	1465	4.43		Ibid.
17957-2	10.85	115.3	2197	0.99	1.49	Sarnthein et al., 1994
GGC-13	10.6	118.283	990	3.54		Miao et al., 1994
SCS-15A	10.4	114.233	1812	0.82	3.51	C. Wang et al., 1986
SCS-15B	10.317	114.183	1500	0.24	1.93	C. Wang and Chen, 1990
SO27-91KL	8.5667	115.7	2060	1.07	7.06	Schönfeld and Kudrass, 1993
17961-2	8.5	112.333	1795	5.17	8.86	Sarnthein et al., 1994
SCS-12	7.7	109.3	543	3.34		Jian et al., 1996
17962-3	7.1833	112.083	1970	7.55	25.12	Sarnthein et al., 1994
NS87-11	7.0167	114.15	2452	1.11	1.61	MOET, 1993
SO58-133KL	6.65	114.717	2136	4.48	19.78	Schönfeld and Kudrass, 1993
RC12-350	6.55	111.217	1950	6.84	12.93	Jian, 1992
SO58-109KL	6.2167	114.067	2792	6.47		Schönfeld and Kudrass, 1993
SO58-110KL	6.1833	114.1	2238	5.83	30.46	Ibid.
17964-2/3	6.1667	112.217	1556	17.54	46.52	Sarnthein et al., 1994
SO58-114KL	6.1	114.233	1929	8.63		Schönfeld and Kudrass, 1993
SO49-136KL	5.9667	114.7	650	4.32		Ibid.
SO49-137KL	5.9333	114.8	220	2.02		Ibid.

ments is most active when drastic sea-level changes take place. During the glacial sea-level lowstand, the increased sedimentation along the shelf break led to an instability of the uppermost continental slope and, hence, to down-slope transport of shelf sediments. This process must be most active when the rapid sea-level rising at the deglaciation brings about slope readjustment and submarine slides (Ross et al., 1994). Submarine slides, being the main process of delta progradation (Kenyon and Turcotte, 1985), are

Table 5
Major rivers emptying the five Western Pacific marginal seas

Marginal sea	River	Water runoff (km^3/yr)	Sediment discharge (10^6 ton /yr)
Okhotsk Sea	Amur R.	57.2	
Japan Sea	No large river		
East China Sea with Yellow Sea and Bohai Gulf	Huanghe (Yellow R.)	42.8	1113.1
	Changjiang (Yangtze)	873.9	472.2
	Liao R.	4.1	18.6
	Luan R.	4.6	19.0
South China Sea	Mekong R.	470	160
	Red R.	123	130
	Pearl R.	84.2	355.2
	Gaoping (Taiwan I.)	9	39
	Zenwen (Taiwan I.)	2	28
Sulu Sea	No large river		

Data from: Fairbridge, 1966; Editorial Committee, Chinese Academy of Science, 1981; Milliman and Meade, 1983; Li et al., 1991.

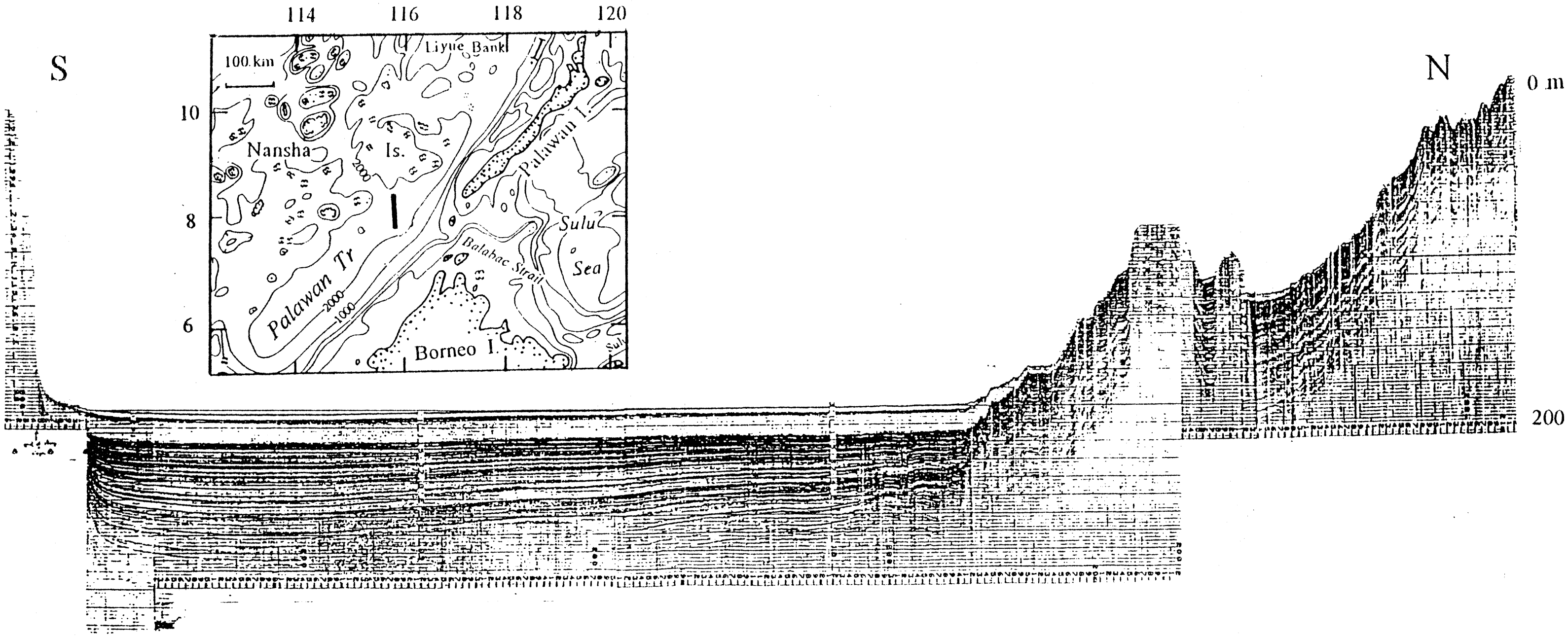

Fig. 7. PARASOUND shallow profile across the Palawan Trough taken by R/V *Sonne* (June 4th, 1994). Note the increasing thickness of sediments towards the bottom of the trough indicating the down-slope transport of sediment.

very frequent in the Western Pacific marginal seas. In the northern slope of the South China Sea, for example, the sediment in the upper slope is significantly thinner than in the lower slope. As shown in Fig. 5, the maximal thickness of the Holocene, with the exception of one single site, is observed in the water depth range between 2000 and 3000 m, i.e., in the lower continental slope above the lysocline. The increased thickness on the lower slope is basically caused by the down-slope transport as evidenced by numerous slumps revealed by shallow-seismic profiling (Sarnthein et al., 1994). A similar pattern is seen in the Palawan Trough, the southern South China Sea, where the shallow-seismic profile clearly shows the increase of deposit thickness from the upper slope of the trough toward its bottom at water depths over 2700 m (Fig. 7).

According to AMS C-14 datings at a number of sites in the South China Sea, large-scale down-slope transport occurred around 13 ka BP. Many sediment cores have a normal age succession in the upper part, whereas the C-14 datings show some reversed order or other abnormality in the lower part older than 13 ka BP. This can be seen in Core SCS90-36 (18º00′N, 111º30′E, w.d. 2050 m, Huang et al., 1997a), Core RC14-85 (15º25′N, 113º49′E, w.d. 1470 m; H. Wang, 1992), Core RC12-350 (6º33′N, 111º13′E, w.d. 1950 m; H. Wang and Jian, 1992) and others. It is believed that submarine slump extensively developed during the last deglaciation with the sea-level rising to the early highstand position. Similar submarine slides have been recorded in the Gulf of Mexico and the North Atlantic (Morton, 1993). The submarine erosion and slumping may reach a much larger scale. Shallow profiling and sediment coring in the Xisha Trough to the north of the Xisha or Paracel Islands, northwestern SCS, has revealed deep erosion of the sea bottom into the Early Pleistocene or even Neogene deposits (Kudrass et al., 1992).

Turbidite sedimentation is another form of down-slope transport in the marginal seas. For example, numerous turbidite layers are intercalated in the late Quaternary hemipelagic mud in the Xisha Trough, South China Sea. The predominance of planktonic foraminifers in the sand fraction of the turbidites implies a reworking of hemipelagic sediments, and the occurrences of mollusk shells and glauconite grains in coarse-grained turbidite indicate down-slope transport from the upper slope or outer shelf (Kudrass et al., 1992), although the finding of shallow-water ostracods in deep-water sediments of the SCS suggests that the down-slope transport of microfossils is not necessarily related to turbidites (Zhou and Zhao, 1999). Turbidites have been found in all the marginal seas in question, but their most frequent occurrences have been reported from the Sulu Sea where the 6-m-thick Holocene in Core SO49-82KL (8ºN, 121ºE, w.d. 4980 m) contains 142 turbidites with graded, finely laminated silt or mud layers (Quadfasel et al., 1990). Such a high frequency of turbidite currents is ascribed to tropical cyclones passing the Mindoro Strait which triggers the overflow of the South China Sea water into the Sulu Sea and enforces the erosion of the sediments and their downward transport. This is one more example of the inter-basinal transport of sediment between marginal seas.

Eolian dust is a negligible component in the modern deep-water sediments of the Western Pacific marginal seas. During glacial times, however, eolian grains may have played a more significant role in some sea areas such as the northeastern slope of the South China Sea (Core 17940, L. Wang et al., 1995). In the Sea of Japan, the ODP core analyses have discovered a prominent shift to higher accumulation rates of eolian-marine deposits near the Gauss/Matuyama boundary, corresponding to the increased aridity of Asia (Dersch and Stein, 1992).

3.3. Biogenic sedimentation and carbonate cycle

3.3.1. Modern distribution

Biogenic components are ubiquitous in the Western Pacific marginal seas. Radiolarians and diatoms predominate in the higher-latitude seas (the Okhotsk Sea and Japan Sea), while foraminifers, coccoliths, pteropods, plus coral, bryozoans and calcareous algae in reef facies dominate in the lower-latitude seas (the East and South China Seas, Sulu Sea, etc.). The Okhotsk and Japan Seas belong to sea areas with the globally highest concentration of opal in sediments, but the opal content is very low in the rest of the marginal seas (Lisitzin, 1972). Fig. 8 shows the general pattern of $CaCO_3$ distribution in the deeper parts (>200 m) of the Western Pacific marginal seas discussed in the present paper. The trend is clear that

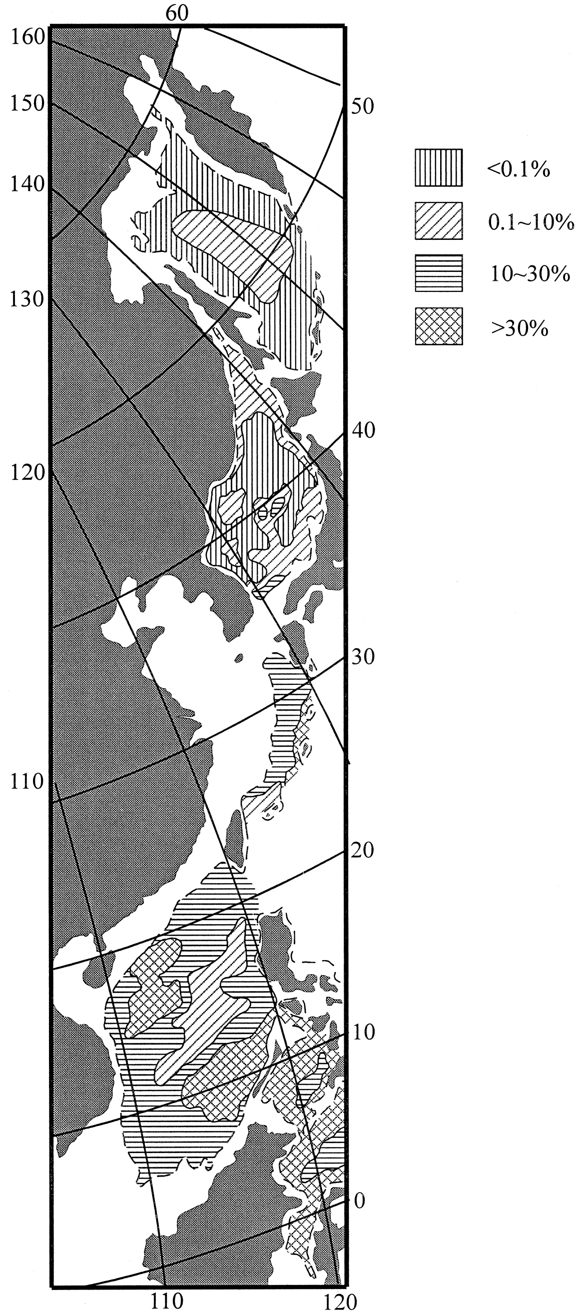

Fig. 8. Distribution of carbonate (%) in surface sediments of the Western Pacific marginal seas deeper than 200 m (based on Likht et al., 1983; Lisitzin, 1972; and new data).

$CaCO_3$ percentage increases toward lower latitudes. In the Sea of Okhotsk carbonate is practically absent in surface sediments of the large area and reaches a few percent only in the shallower central part remote from the coast. Carbonate content is very low in the northern part of the Sea of Japan and increases southwards, exceeding 10% in the Yamato Rise and near the Tsushima Strait. The carbonate content is higher in the Okinawa Trough, East China Sea, varying between 10 and 30% in most of the area and rising to 50–60% near coral reefs. It decreases to below 10% in the southernmost area near Taiwan. In the SCS carbonate exceeds 10% everywhere (except in the central basin below CCD, about 3500 m) and becomes the dominant component of surface sediments in reef areas near Xisha, Zhongsha and Nansha Islands. The highest $CaCO_3$ values occur in the Sulu Sea where $CaCO_3$ declines below 30% only in the deepest part (Fig. 8).

3.3.2. Carbonate cycles

The Quaternary carbonate cycles in the Equatorial Pacific have been extensively discussed in the paleoceanographic community (e.g., Arrhenius, 1952; Berger, 1973, 1992; Luz and Shackleton, 1975; Farrell and Prell, 1989; Le and Shackleton, 1992), but not much has been published for its marginal seas except for the South China Sea (Rottmen, 1979; P. Wang et al., 1986, 1995; Thunell et al., 1992; Bian et al., 1992; H. Wang and Jian, 1992; Li, 1993; Zheng et al., 1993; Schönfeld and Kudrass, 1993; Miao et al., 1994; Chen et al., 1997) and the Sulu Sea (Linsley, 1991; Miao et al., 1994). Nevertheless, the high sedimentation rates and the morphological and climatic variety of the marginal seas provide an excellent opportunity to explore the factors controlling carbonate content in glacial cycles, and a comparison of carbonate cycles in the marginal seas will give insight into marine chemistry, productivity, and land erosion of the marginal seas. Representative curves of the late Quaternary carbonate content in five Western Pacific marginal seas are compiled in Fig. 9.

In the Sea of Okhotsk, the carbonate content remains extremely low through the glacial cycles, and 'spikes' in the carbonate curve occur only at oxygen isotope stages 1 and 3, coinciding with those of opal (Core K-105, 52º53′N, 150º24′E, w.d. 1130 m; Fig. 9A, Gorbarenko, 1991a,b). This suggests that sediments rich in biogenic carbonates, opal and organic carbon have been accumulated in the Sea of

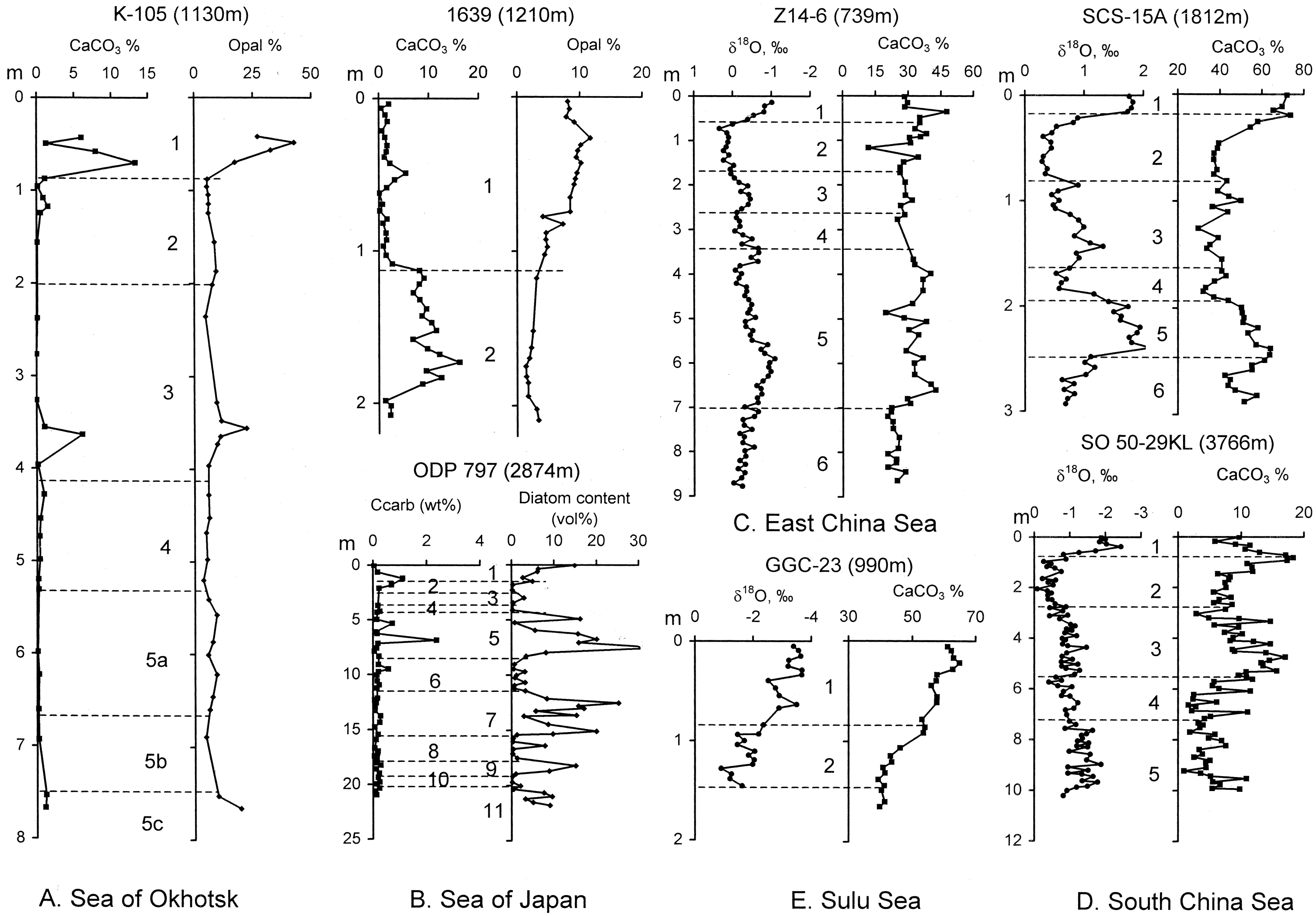

Fig. 9. $CaCO_3$ curves from various Western Pacific marginal seas. (A) Sea of Okhotsk, Core K-105 (after Gorbarenko, 1991a). (B) Sea of Japan, Core 1639 (after Gorbarenko, 1987) and ODP 797 (carbon content of carbonate is shown; after Tada et al., 1992). (C) East China Sea, Core Z14-6 (after P. Wang, 1990). (D) South China Sea, Core SCS-15A (after C. Wang et al., 1986) and Core SO 50-29KL (after Zheng et al., 1993). (E) Sulu Sea, Core GGC-23 (after Miao et al., 1994). Numbers denote oxygen isotope stages.

Okhotsk only during warm stages, and the trend of down-core variations is very close to those of the 'northwest Pacific type' of carbonate cycles (Haug et al., 1995).

The carbonate cycle is very different in the Sea of Japan. Also with a very low background value, the higher percentages of carbonate occur in the glacial intervals (oxygen isotope stages 2, 6 and the later part of stage 5), as seen in Core 1639 (38º38′N, 137º13′E, w.d. 1210 m; Gorbarenko, 1987) and ODP Site 797 (38º37′N, 134º32′E, w.d. 2874 m; Tada et al., 1992) (Fig. 9B). Moreover, the carbonate maxima are out of phase with those of opal which increases in warm and decreases in cold stages. Carbonate analyses of a large number of cores from the Sea of Japan by Russian scientists have found the same trend of down-core variations, showing a peak late in stage 2 (Gorbarenko, 1987). Therefore, the carbonate cycles observed in the Japan Sea can not be ascribed to surface productivity and the question of the controlling mechanism remains open.

More than ten years ago, the late Quaternary carbonate curve in the South China Sea was found to be of the 'Atlantic type' running roughly parallel with oxygen-isotopic curves (P. Wang et al., 1986). This was confirmed by curves at other sites above the lysocline in the South China Sea (C. Wang et al., 1986; Thunell et al., 1992; Bian et al., 1992; Li, 1993; Zheng et al., 1993; Miao et al., 1994; P. Wang et al., 1995) and in the East China Sea (Yan, 1989; P. Wang, 1990), while curves of the 'Pacific type' have been found at sites below the lysocline (Fig. 9C, D; P. Wang et al., 1995). The same has been recorded in the Sulu Sea, with carbonate curves of the 'Atlantic type' above the lysocline (e.g., Core GGC-23, 8º09′N, 118º34′E, w.d. 990 m; Miao et al., 1994) and those of the 'Pacific type' below the lysocline (e.g., Core SO58-67KL, 8º50′N, 121º20′E, w.d. 3350 m; Vollbrecht and Kudrass, 1990). Thus, the two-type model of carbonate cycles seems to be common to all the lower-latitude marginal seas, and a total of four types of carbonate curves can be recognized in the five Western Pacific marginal seas (Fig. 10): (A) Northwestern Pacific type (Fig. 9A; Fig. 10A); (B) Japan Sea type (Fig. 9B; Fig. 10B); (C) Atlantic type (Fig. 9C, E and D, SCS-15A; Fig. 10C); (D) Pacific type (Fig. 9D, SO50-29KL; Fig. 10D).

3.3.3. Controlling factors

The variety of carbonate cycle types is largely dictated by the origin and characteristics of the deep water masses of the individual basins which in turn depend on the basin morphology. The Sea of Okhotsk with its sill depth at about 2000 m and an S/B ratio of 0.59 is well connected with the ocean, and the deep waters exchange well with those in the NW Pacific. In recent studies on variations of carbonate flux on the Emperor Seamount Ridge, NW Pacific, the 'northwestern Pacific type' of carbonate curves was discovered, with enhanced carbonate accumulation rates during interglacial stages (Haug et al., 1995), and a high-resolution study shows that the increase in productivity occurs during deglaciation rather than in the Holocene (Keigwin et al., 1992). Exactly the same has been found in the Sea of Okhotsk. In five sediment cores retrieved from its central part by the Russian R/V *Kallisto* the carbonate, opal and organic carbon spikes occur at stages 1 (early part, close to deglaciation), 3 and 5 (Gorbarenko et al., 1988), suggesting that the Sea of Okhotsk shows also carbonate cycles of the 'Northwestern Pacific type' (Fig. 9A, Fig. 10A) similar to the Emperor Seamount. The low content of biogenic component in sediments during the glacial is probably related to the sea ice coverage. Only during warmer periods can the higher productivity result in carbonate and opal accumulation as observed in the Northwestern Pacific and in the Sea of Okhotsk. Higher productivity may be related to the strengthened upwelling during the interglacial as a consequence of the global 'Conveyor Belt' of thermohaline circulation (Broecker, 1991).

The carbonate cycles in the Sea of Japan are different. Due to the extremely shallow sill depth (130 m) and the low S/B ratio (0.03), the deeper waters in the Sea of Japan are not of a Pacific origin. Instead, the dense water formed in the northern half of the sea under low temperature and high wind stress sinks down to generate the very homogeneous Sea of Japan Proper Water which occupies the basin below the upper layer (see Section 2). The turnover time of the water is only about 100 years, and the bottom water temperature is as low as 0–1ºC. Therefore, the Sea of Japan is characterized by a very shallow calcite lysocline (about 1200–1400 m) and CCD (about 1400–1600 m) (Chen et al., 1995). This

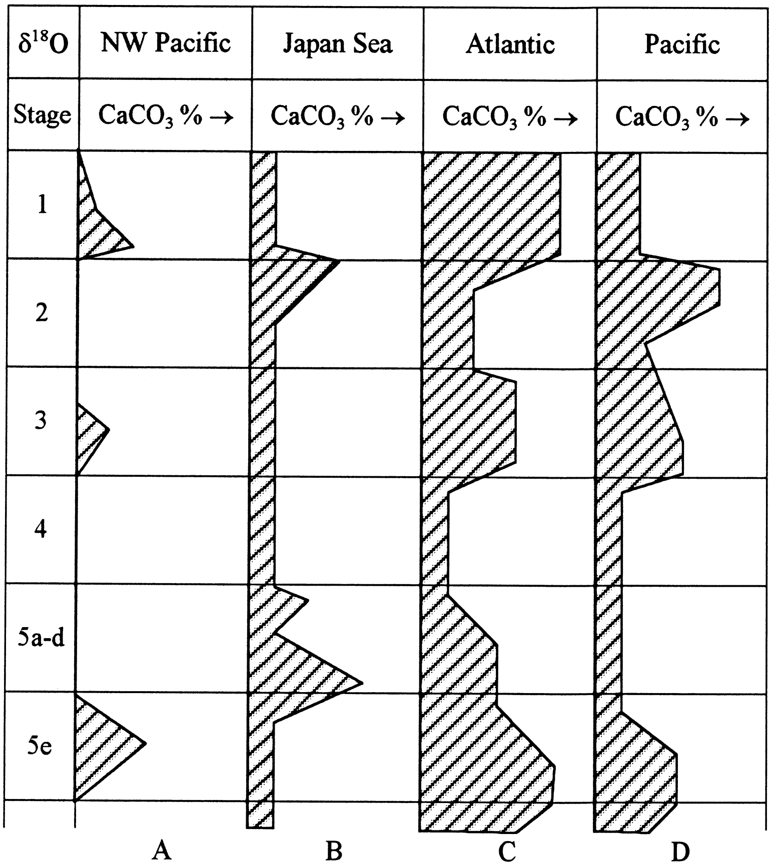

Fig. 10. Diagram showing four types of $CaCO_3$ curves in the Western Pacific marginal seas: (A) Northwestern Pacific type; (B) Japan Sea type; (C) Atlantic type; (D) Pacific type.

explains the poor carbonate preservation in the Sea of Japan. Although it is yet unclear whether the carbonate peak late in oxygen isotope stage 2 is related to the stratification of the water column and the elevated alkalinity of the bottom water (Gorbarenko, 1987), or to the calcareous plankton bloom resulting from the changes in circulation (Oba et al., 1991; Tada et al., 1992), the carbonate cycles in the Sea of Japan differ from those in the Equatorial and Northwestern Pacific, as the carbonate peaks are out of phase with those of opal or organic carbon (Fig. 9B; Gorbarenko, 1991a,b), and no carbonate maxima are recorded before the oxygen isotope stage 5 (Tada et al., 1992).

The carbonate cycles of the East and South China Seas and the Sulu Sea are similar, but their bottom waters have different origins. As mentioned above, the bottom waters in the Sulu Sea originate from the SCS, flowing through the Mindoro Strait with a sill depth of 420 m, whereas the bottom waters of the South China Sea come directly from the Western Pacific through the Bashi Strait where the sill depth is 2600 m. Therefore, the bottom water temperature is as high as 10ºC in the Sulu Sea, but only 2ºC in the South China Sea, and this leads to a better preservation of carbonate in the Sulu Sea. The calcite lysocline and CCD are about 3000 m and 3500 m in the South China Sea (P. Wang et al., 1995), but 3800–4000 m and 4500–4800 m in the Sulu Sea (Exon et al., 1981; Linsley et al., 1985).

The existence of two types of carbonate cycles in these low-latitude seas is of particular interest and deserves a special discussion in a separate paper. Since the $CaCO_3$ curve embodies the signals of car-

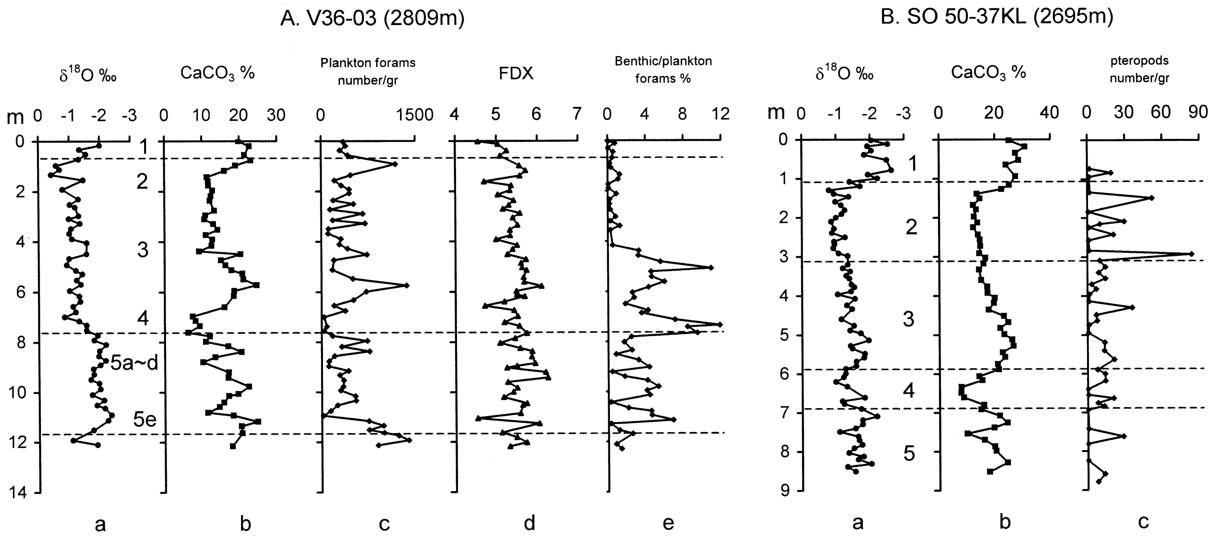

Fig. 11. Comparison of downcore variations of $CaCO_3$ (%) with those of dissolution proxies in the northern South China Sea. (A) Core V36-03 (after P. Wang et al., 1995); (B) Core SO50-37KL (after L. Wang et al., 1997).

bonate production, deep-sea dissolution and dilution by non-carbonate deposits (Berger, 1992), it can not be attributed to any one single environmental factor. Fig. 11 shows the relationship between $CaCO_3$ percentage, aragonite preservation (pteropod abundance), and proxies of carbonate dissolution, such as fragment ratio of foraminifers, benthic/planktonic foraminiferal ratio, dissolution index of foraminiferal tests, in two cores taken from the northern South China Sea above the lysocline (V36-03, SO50-37KL). Both the curves of foraminiferal dissolution index and benthic/planktonic ratio are of a typical 'Pacific type'. Moreover, the number of pteropod specimens per gram sediment also displays 'Pacific-type' cycles (Fig. 11). Recent studies on carbonate preservation of two other cores from the northern South China Sea since 25 ka (Core SCS90-36, Core 31KL; Chen et al., 1997) confirm the occurrence of maximal preservation during the later half of the glacial which is typical of 'Pacific-type' carbonate cycles. The apparent 'Atlantic-type' carbonate percentage curve observed in the South China Sea was interpreted as a stacking of dissolution and dilution cycles (P. Wang et al., 1995), but recent calculations show that the trend of carbonate accumulation rates vary from area to area (Table 6; Huang, 1997) and can not be ascribed solely to the dilution effect by terrigenous debris. In the northern South China Sea, the accumulation rate is higher during the warm stages for the sites above the lysocline, whereas in the southern part it is higher in the cool stages, with the exception of the southernmost station (Core 17961). This again is a specific feature of marginal seas where the biogenic production is subject to remarkable temporal as well as spatial variations. Further studies are needed to decipher the observed variety of carbonate cycles in the Western Pacific marginal seas.

3.4. Low-oxygen deposits

The oxygen content in the water column of marginal seas is highly variable in the enclosed-basin type and is very sensitive to sea-level changes during glacial cycles. Among the Western Pacific marginal seas, the Sea of Japan and the Sulu Sea are distinguished by their extent of isolation where low-oxygen or anoxic conditions were present during glacial periods. When the Sea of Japan was almost isolated during the LGM, the absence of deep-water exchange and the input of fresh water to the basin resulted in a strong stratification of the water column leading to the deposition of laminated sediments (Oba et al., 1991). Similar cases have been recorded throughout the glacial periods, and numerous dark–light cycles in sediments of a Milankovitch type and

Table 6
Carbonate accumulation rates (g cm^{-2} ka^{-1}) during various oxygen isotope stages in the South China Sea

Core	Location (°)		Water depth (m)	Oxygen isotope stages				
	N	E		stage 1	stage 2	stage 3	stage 4	stage 5
Northern part								
17949	17.35	115.17	1334	1.72	1.16	0.93	0.50	1.56
17941	21.52	118.48	2201	0.62	0.33	0.64	0.10	0.64
SO50-37KL	18.92	115.77	2695	1.81	1.36	1.04	0.76	
17948	16.72	114.90	2855	1.27	0.97	1.18	0.85	1.52
SO50-29KL	18.33	115.98	3766	0.47	0.92	0.78	0.15	
Southern part								
17954	14.77	111.53	1517	1.37	1.59	0.64	0.63	1.14
SCS-15A	10.40	114.23	1812	0.56	1.65	0.57	0.56	0.33
17957	10.85	115.30	2197	0.65	0.93	0.26	0.47	0.69
17955	14.12	112.18	2393	1.16	1.19	0.60	0.67	0.95
8357	13.48	118.02	3949	0.25	0.65	0.21	0.44	
17961	08.50	112.33	1795	1.39	0.98	0.89	0.53	0.57

Data from Huang, 1997, based on preliminary data from: C. Wang et al., 1986; Zheng et al., 1993; Li, 1993; Sarnthein et al., 1994.

of a monsoon-related origin were discovered in ODP cores (Follmi et al., 1992; Tada et al., 1992). In the Sulu Sea, the enhanced isolation of the basin and reduced surface salinity during glacial times resulted in stagnation of deep water and an expansion of the mid-water oxygen minimum layer (Linsley et al., 1985).

Because of its sensitivity to minor changes in oxygen content the benthic foraminiferal fauna provides a better indicator of oxygenation of bottom waters. An example is the southern Okinawa Trough where the increased proportion of low-oxygen-tolerating species in benthic foraminifera indicates lowered bottom-water oxygen conditions during the last deglaciation (Jian et al., 1996).

Some important aspects of sedimentology in the Western Pacific marginal seas, such as volcanoclastic sediments, are not touched here. However, the above discussion is sufficient to demonstrate the major specific features of the sedimentological response of the marginal seas to glacial cycles.

4. Paleoceanographic response

4.1. Paleogeographic changes

The Last Glacial Maximum (LGM) is characterized by the development of enormous ice sheets. The last glacial Laurentide ice sheet in North America, for instance, was similar in area to the present Antarctic ice sheet, and the Scandinavian ice sheet then covered all the Barents Sea and the Kara Sea. However, there was no continental ice cap developed in northeastern Asia (Frenzel et al., 1992), and the 'East Siberian Arctic Shelf Ice Sheet (ESASIS) Hypothesis' and the 'Marine Ice Transgression Hypothesis (MITH)' (Hughes and Hughes, 1994) are not supported by the paleontological findings (Rutter, 1995; Sher, 1995). Instead, the emergence of vast shelf areas of the marginal seas was the most prominent geographic change in the Western Pacific region at the LGM.

During the LGM, the shelf seas were exposed subaerially and covered by a network of river channels as reported from the Java Sea (Umgrove, 1949) and Yellow Sea (Qin et al., 1986), or occupied by a lake, as in the case of the Gulf of Carpentaria (Torgersen et al., 1983). Of the numerous continental shelves of the Western Pacific, three are most extensive (Fig. 12): (1) the East China Sea Shelf with a total area of 850,000 km^2; (2) the Sunda Shelf or Great Asian Bank, including the southern part of the South China Sea with the Gulf of Thailand, and the Java Sea, with a total area of 1,800,000 km^2; (3) the Sahul Shelf or Great Australian Bank, including the Timor Sea Shelf or Sahul Shelf s.str., the Arafura shelf and the Gulf of Carpentaria, with a total area

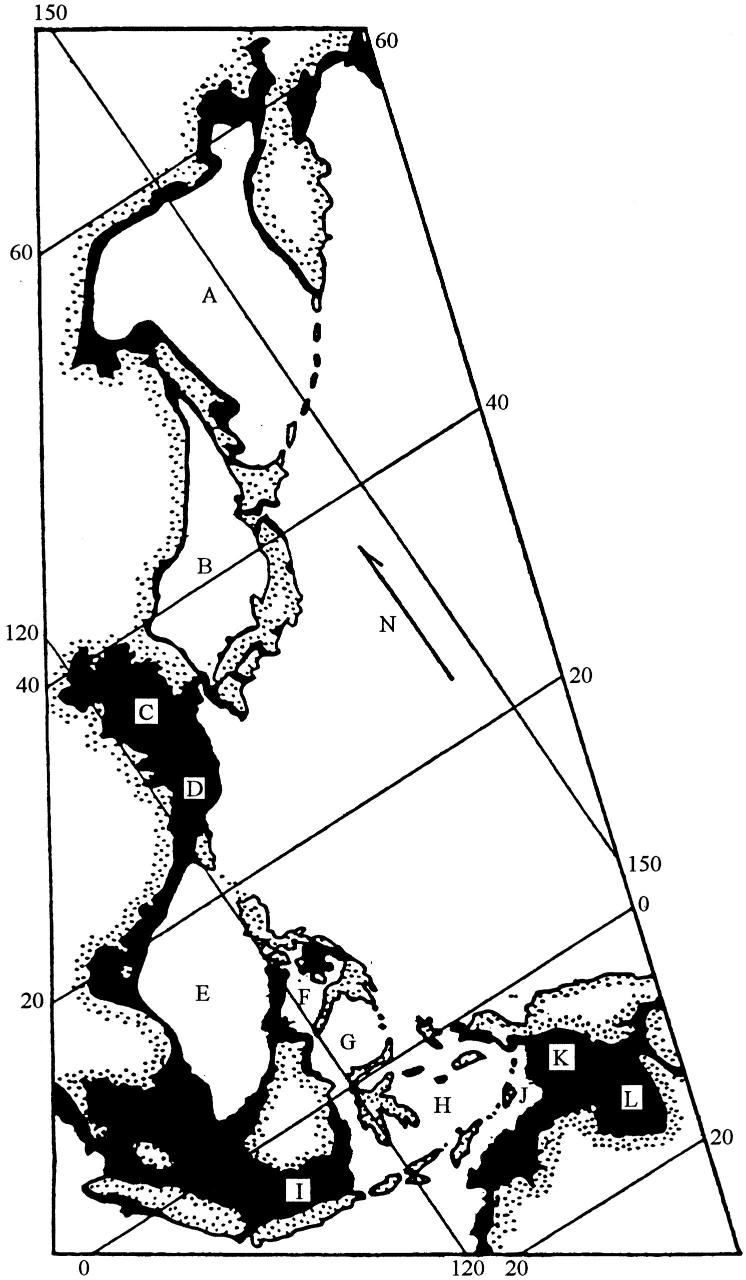

Fig. 12. Emerged shelves (solid areas) in the Western Pacific marginal seas at the LGM (A) Okhotsk Sea, (B) Sea of Japan, (C) Yellow Sea and Bohai Gulf, (D) East China Sea, (E) South China Sea, (F) Sulu Sea, (G) Celebes Sea, (H) Banda Sea, (I) Java Sea, (J) Timor Sea, (K) Arafura Sea, and (L) Gulf of Carpentaria.

of 1,230,000 km^2. These three major shelves sum to ca. 3,900,000 km^2 and all were exposed during the LGM. The large-scale changes in sea/land area and the consequent rapid migration of the coastline in glacial cycles must have had profound environmental significance (P. Wang, 1991; UNESCO/IOC, 1995). For example, within some 8000 years of the last deglaciation, the coastline migrated about 1200 km landwards from the western border of the Okinawa Trough to the western coast of the modern Bohai Gulf, suggesting a coastline retreat of >0.4 m per day in average. The drastic reduction in sea area in glacial time must also have had remarkable influence on the vapor transfer from the sea to the land.

4.2. Enhanced seasonality in marginal seas

On the basis of micropaleontological data, the CLIMAP studies concluded that the "ice-age ocean was strikingly similar to the present ocean in at least one respect: large areas of the tropics and subtropics within all oceans had sea-surface temperatures as warm as, or slightly warmer than, today" (CLIMAP, 1981, p. 9). Recent studies in the Western Pacific using the modern analogue technique (MAT) also "indicate that tropical SSTs differed by less than 2°C from present", implying the stability of the Western Pacific warm pool within the glacial cycles (Thunell et al., 1994). These conclusions, however, are challenged by recent studies. Since the marginal seas provide much higher sedimentation rates and, hence, much finer stratigraphic resolution than in the open ocean, the paleotemperature data yielded by the extensive paleoceanographic studies in the Western Pacific marginal seas may throw new light on the above questions. Available paleo-SST data from the South and East China Seas, Sulu Sea and the adjacent West

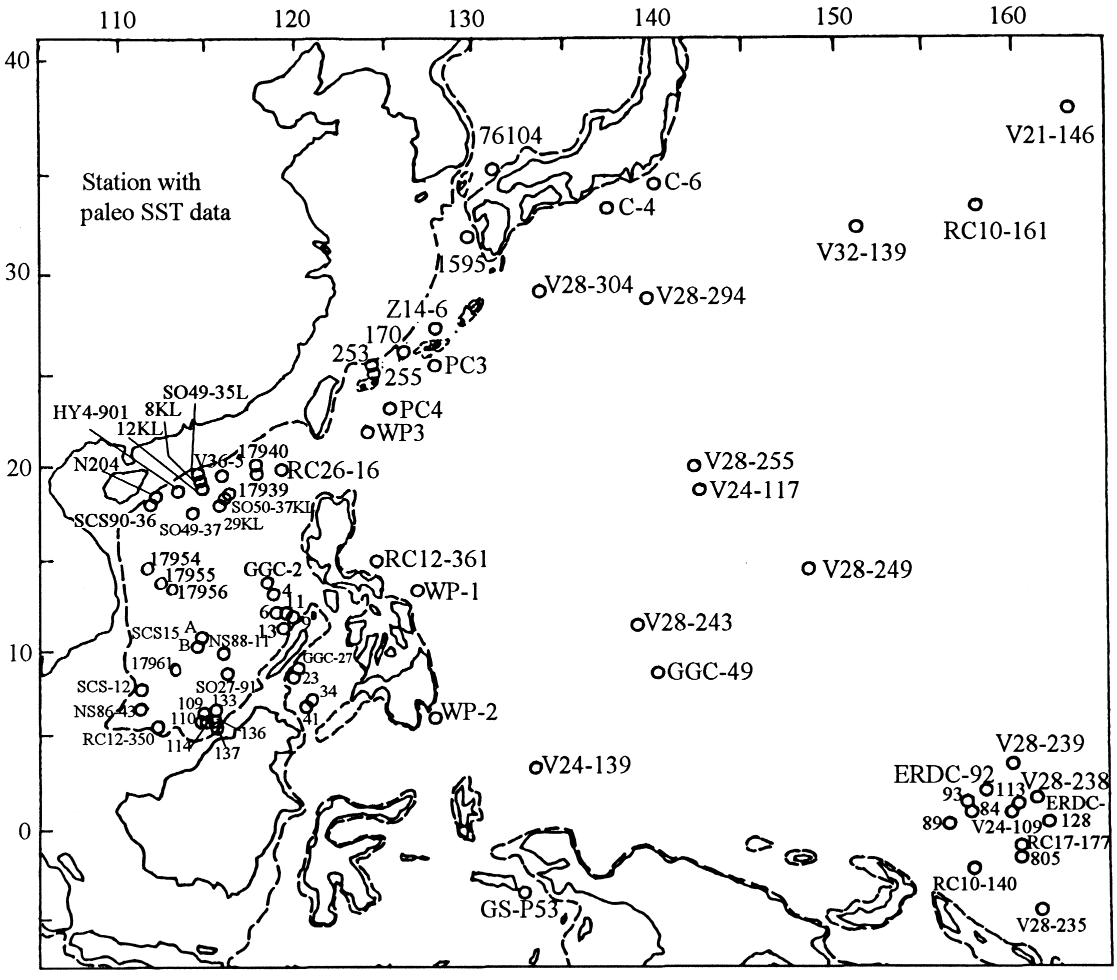

Fig. 13. Location map of sites with paleo-SST data.

Table 7
Data sources of paleo-SST and oxygen-isotopic values in the Western Pacific at the Last Glacial Maximum used in Fig. 14

Core	Location	Water depth (m)	Foraminiferal SST	$\delta^{18}O$	Reference
V21-146	37º41′N, 163º02′E	3968	•		Thompson, 1981
76104	35º17′N, 131º07′E	125		•	Gorbarenko, 1993
KH79-3-6 (C-6)	34º43′N, 140º33′E	2020		•	Oba et al., 1983; Chinzei et al., 1984
KH79-3-4 (C-4)	33º09′N, 137º42′E	3353		•	Chinzei et al., 1984
1595	32º06′N, 129º16′E	660		•	Gorbarenko, 1991a,b; Gorbarenko, 1993
RC10-161	32º05′N, 158º00′E	3587	•		Thompson, 1981
V32-139	31º34′N, 151º05′E	2030	•		ibid.
V28-304	28º32′N, 134º08′E	2942	•		ibid.
V28-294	28º26′N, 139º58′E	2308	•		ibid.
Z14-6	27º07′N, 127º27′E	739		•	Cang and Yan, 1992
170	26º38′N, 125º48′E	1470	•		Li et al., 1997
253	25º34′N, 123º01′E	839	•		ibid.
RN89-PC3	25º21′N, 127º29′E	2255	•	•	Ahagon et al., 1993; Xu and Oda, 1995
255	25º12′N, 123º06′E	1575	•	•	Li et al., 1997
RN87-PC4	23º50′N, 124º24′E	2488	•	•	Ahagon et al., 1993; Xu and Oda, 1995
WP3	22º09′N, 122º57′E	2700	•	•	Thunell et al., 1994
17940	20º07′N, 117º23′E	1727	•	•	L. Wang et al., 1999
V28-255	20º06′N, 142º27′E	3261	•		Moore et al., 1980
17939	19º58′N, 117º27′E	2474		•	L. Wang et al., 1999
RC26-16	19º35′N, 118º02′E	2912	•	•	Li, 1995
SO49-3KL	19º35′N, 114º12′E	713		•	Schönfeld and Kudrass, 1993
V36-5	19º26′N, 115º55′E	2332	•		Wang and Wang, 1990
SO49-8KL	19º11′N, 114º12′E	1040	•	•	Wang and Wang, 1990; Schönfeld and Kudrass, 1993
SO49-12KL	19º01′N, 114º30′E	1532		•	Schönfeld and Kudrass, 1993
SO50-37KL	18º55′N, 115º46′E	2695		•	Winn et al., 1992; Zheng et al., 1993.
HY4-901	18º49′N, 113º28′E	1120		•	Li et al., 1996
V24-117	18º36′N, 142º22′E	3706	•		Thompson, 1981
SO50-29KL	18º20′N, 115º59′E	3766		•	Winn et al., 1992; Zheng et al., 1993
N204	18º13′N, 110º06′E	180	•	•	Gao et al., 1992
SCS90-36	18º00′N, 111º30′E	2050		•	Huang et al., 1997a
SO49-37KL	17º49′N, 112º47′E	2004		•	Schönfeld and Kudrass, 1993
RC12-361	15º06′N, 124º08′E	3528	•		Moore et al., 1980
17954	14º48′N, 111º32′E	1520		•	L. Wang et al., 1999
V28-249	14º35′N, 147º52′E	2569	•		Thompson, 1981
17955	14º07′N, 112º11′E	2393		•	L. Wang et al., 1999
17956	13º51′N, 112º35′E	3388		•	ibid.
WP1	13º47′N, 125º34′E	2208	•	•	Cang and Yan, 1992; Thunell et al., 1994
GGC2	13º37′N, 117º41′E	4010	•		Thunell et al., 1992; Miao et al., 1994
GGC4	12º39′N, 117º56′E	3530	•	•	ibid.
GGC6	12º09′N, 118º04′E	2975	•	•	ibid.
GGC11	11º53′N, 118º20′E	2165	•	•	ibid.
GGC9	11º38′N, 118º38′E	1465	•		ibid.
V28-243	11º04′N, 138º32′E	2129	•		Moore et al., 1980
17957	10º54′N, 115º18′E	2195		•	L. Wang et al., 1999
GGC13	10º31′N, 118º17′E	990	•	•	Thunell et al., 1992; Miao et al., 1994
SCS-15A	10º24′N, 114º14′E	1812		•	C. Wang et al., 1986
SCS-15B	10º19′N, 114º11′E	1500		•	C. Wang and Chen, 1990
NS88-11	9º56′N, 115º37′E	995	•		Li et al., 1992
SO27-91KL	8º34′N, 115º42′E	2060		•	Schönfeld and Kudrass, 1993
GGC27	8º30′N, 118º15′E	2030	•		Miao et al., 1994.
17961	8º30′N, 112º20′E	1795		•	L. Wang et al., 1999
GGC23	8º09′N, 118º34′E	990	•		Miao et al., 1994

Table 7 (continued)

Core	Location	Water depth (m)	Foraminiferal SST	$\delta^{18}O$	Reference
SCS-12	7°42′N, 109°18′E	543	•	•	Jian et al., 1996
GGC41	7°13′N, 119°32′E	4203	•		Miao et al., 1994
NS86-43	7°10′N, 110°20′E	1763	•		Li et al., 1992
GGC34	6°54′N, 119°10′E	2970	•		Miao et al., 1994
SO49-133KL	6°39′N, 114°43′E	2136		•	Schönfeld and Kudrass, 1993
RC12-350	6°33′N, 111°13′E	1950	•	•	Jian, 1992
WP2	6°20′N, 136°26′E	1580		•	Thunell et al., 1994
SO49-109KL	6°13′N, 114°04′E	2792		•	Schönfeld and Kudrass, 1993
SO49-110KL	6°11′N, 114°06′E	2238		•	ibid.
SO49-114KL	6°06′N, 114°14′E	1929		•	ibid.
SO49-136KL	5°58′N, 114°42′E	650		•	ibid.
SO49-137KL	5°56′N, 114°48′E	220		•	ibid.
V24-139	3°31′N, 132°26′E	3355	•		Thompson, 1981
V28-239	3°15′N, 159°11′E	3490	•	•	ibid.
RC17-177	1°45′N, 159°27′E	2600		•	Linsley and Dunbar, 1994
ERDC-84P	1°25′N, 157°15′E	2339		•	Wu et al., 1991
ODP 805	1°14′N, 160°32′E	3187		•	Berger et al., 1993
V28-238	1°01′N, 160°19′E	3125	•		Thompson, 1981
V24-109	0°26′N, 158°48′E	2367	•		ibid.
ERDC-128	0°00′, 161°24′E	3700		•	Thunell et al., 1994
ERDC-89P	0°0.2′S, 155°52′E	193		•	Wu et al., 1991
ERDC-113P	1°38′S, 159°13′E	2158		•	ibid.
ERDC-93P	2°15′S, 157°01′E	1604		•	ibid.
RC10-140	2°39′S, 156°59′E	1679	•		Thompson, 1981
G5-P53	3°36′S, 132°10′E	1991		•	Thunell et al., 1994
V28-235	5°27′S, 160°29′E	1746	•		Moore et al., 1980

Pacific during the LGM (Fig. 13, Table 7) are summarized in Fig. 14a,b. The paleo-SST estimations are based on planktonic foraminiferal census using the transfer function FP12-E developed for the Western Pacific (Thompson, 1981).

As seen from the figures, the LGM summer SST for the South China and Sulu Seas between 5° and 20°N ranges from 25.6°C to 29.0°C, averaging 27.8°C, while in the open Western Pacific at the same latitudes it ranges from 27.1°C to 29.6°C with an average of 28.7°C, very close to that in the marginal seas (Fig. 14b). The LGM winter SSS varies from 16.0°C to 24.0°C in the South China and Sulu Seas, averaging 21.1°C, and from 23.8°C to 28.0°C in the open ocean, averaging 26.0°C, or 4.9°C higher than that in the marginal seas (Fig. 14a). Thus, the winter SST at the LGM was much cooler in the Western Pacific marginal seas than in the open ocean, whereas in summer the SST was similar in the marginal seas and ocean, resulting in a much more intensive seasonality during the LGM in the marginal seas (Fig. 14c). In fact, the winter SST at the LGM was at least 3–4°C lower in the South China Sea and Sulu Sea than in the open Pacific (Fig. 14a), and the LGM seasonality is about 4°C higher then in the ocean (Fig. 14c).

In recent years, the different results of paleo-SST reconstructions led to new efforts to improve the transfer function technique and to a debate whether the paleoecological transfer function technique is applicable to the tropics (Anderson and Webb, 1994). Therefore, independent paleo-SST proxies based on organic and isotopic geochemistry are used to verify our conclusions drawn from micropaleontology. As an organic-geochemical proxy of paleo-temperature, the ratio of unsaturated long-chain alkenones ($U^{k'}_{37}$) biosynthesized by coccolithophorids is closely correlated with SST. Up to now, there are at least four cores analyzed for $U^{k'}_{37}$ measurements in the South China Sea, and the resulting LGM/Holocene SST contrast is 4°C to 4.5°C in the north and 2.5°C in the south, all exceeding that in the open Pacific (only 0.7°C) (see Table 8). This agrees well with our

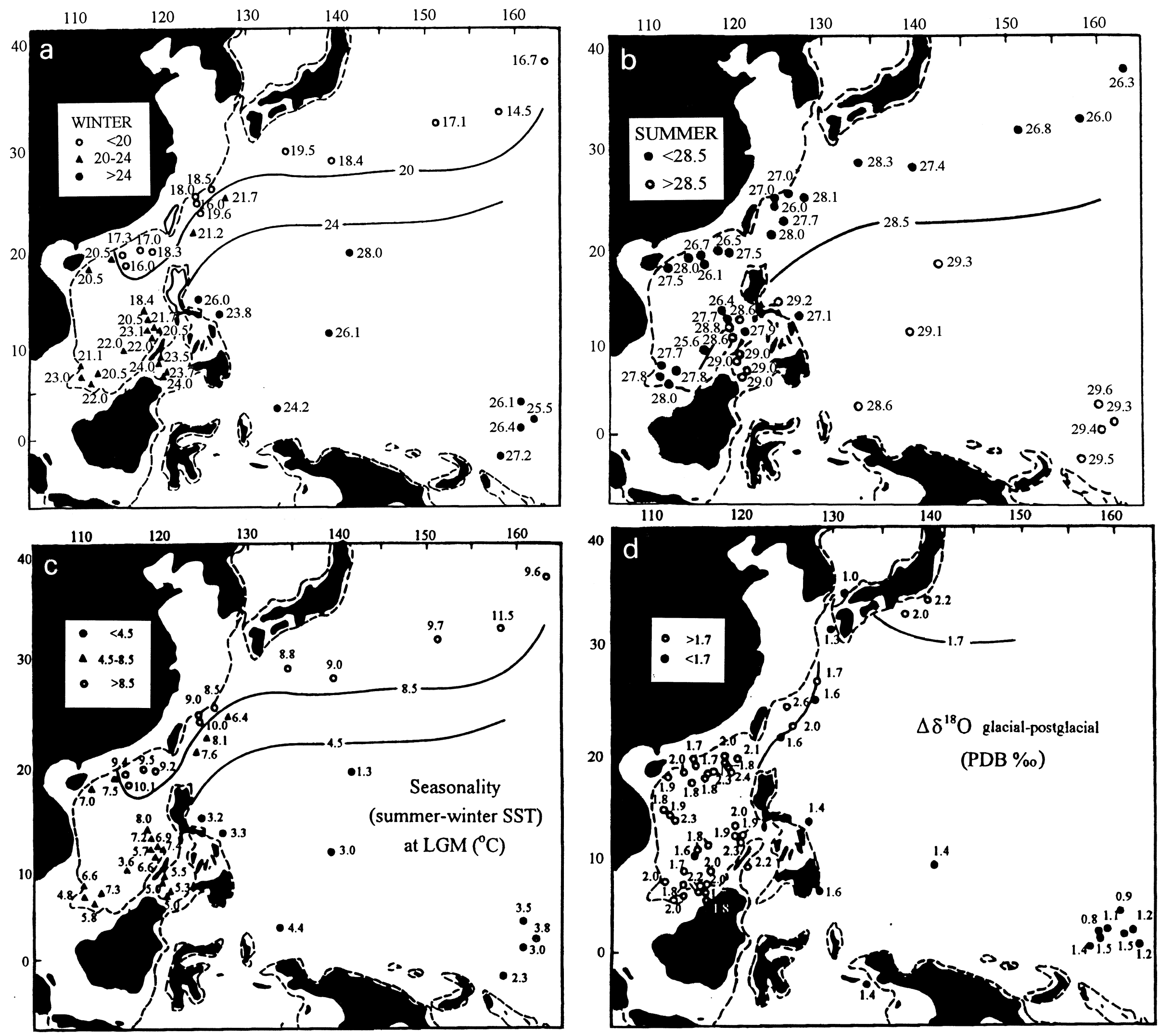

Fig. 14. Sea surface temperature in the low- and middle-latitude Western Pacific and marginal seas at the Last Glacial Maximum. The paleo-SST estimations are based on census of planktonic foraminifers using transfer function FP 12-E (see Table 7 for data sources). (a) Winter sea surface temperature. (b) Summer sea surface temperature. (c) Seasonality in SST (summer SST minus winter SST). (d) LGM/Holocene difference in oxygen isotope values of shallow-dwelling planktonic foraminifers.

Table 8
$U_{37}^{k'}$ SST estimates for the South China Sea and the Western Pacific

Sea	Site	Location	LGM/modern SST contrast	Reference
South China Sea	17940	20°07′N, 117°23′E	4.5°C	Pelejero et al., 1996
	SCS90-36	18°00′N, 111°30′E	4°C [a]	Huang et al., 1997b
	SO50-31KL	18°45′N, 115°52′E	4°C	Huang et al., 1997a
	17961	08°30′N, 112°20′E	2.5°C	Pelejero et al., 1996
West Pacific	W8402A-14GC	00°57′N, 138°57′E	<2.0°C (0.7°C)	Lyle et al., 1992

[a] Contrast between the modern and 14-ka records.

micropaleontology-based conclusions. On the other hand, different transfer functions may result in different paleo-SST estimations. The glacial/Holocene SST contrast in Core 17940 from the northern South China Sea, however, remains almost unchanged, whether the newly developed SIMMAX-28 transfer function or the transfer function FP-12E are used for estimations (Pflaumann and Jian, 1999).

Oxygen isotope data for the late Quaternary are now available from many sites in the Western Pacific marginal seas, in particular the South China Sea. As seen from the LGM-Holocene changes in the oxygen isotope of shallow-dwelling planktonic foraminifers (*Globigerinoides sacculifer* or *G. ruber*) (Fig. 14d, Table 7), the contrast is again much more significant in the marginal seas than in the open ocean at the same latitudes. The glacial–postglacial difference in δ^{18}O is less than 1.7‰ in the open ocean south of 30ºN, while it exceeds 1.7‰ in the marginal seas at the same latitudes. Although the greater difference in oxygen isotopic value might be partly caused by salinity changes in the marginal seas, there is no contradiction between the δ^{18}O data and the trend of paleo-SST changes discussed above.

4.3. Climate impact of changes in marginal seas

4.3.1. Asian monsoon and moisture transfer

The amplifying role of marginal seas in their environmental response to the glacial cycles is of great significance for climate variations in Asia, including the East Asian monsoon and inland aridity, for the variability of the warm pool and for the 'tropical paleoclimate enigma' (Anderson and Webb, 1994). Seasonality in the Western Pacific marginal seas is closely related to the East Asian monsoon. As shown by modern monsoon studies, in winter the northerly air flow from the cold Siberian high pressure cell crosses the Equator above the South China Sea area and becomes the strongest winter monsoon flow in the world (Chen et al., 1991). In the northern South China Sea, the content of eolian dust (L. Wang et al., 1995) and pollen from the northern vegetation types (Sun and Li, 1999) drastically increased in the LGM deposits, indicating a considerable intensification of the winter monsoon during the glaciation which led to a decrease of winter SST in the marginal seas and strengthened seasonality there. Thus, the enhanced seasonality at the LGM should be ascribed to the Eastern Asian monsoon and the semi-enclosed nature of the marginal seas (P. Wang, 1995a). Its absence is to be expected in the open Pacific outside of the monsoon regime.

The size reduction of marginal seas and the SST decline there must have effected the water balance in the region. Since moisture in the East Asian continent, and China in particular, is mainly supplied by the southern (boreal summer) monsoon, while precipitation in northern Australia and the islands between Australia and the Asian continent is provided mainly by the northern (boreal winter) monsoon, the seasonal difference in SST pattern in the marginal seas should have a different climate impact on the two areas. In general, the evaporation from sea is much higher than from land, and the evaporation from the sea surface is related to the SST, hence the glacial reduction of sea area and SST should decrease the vapor supply from the sea surface. Given that wind direction and intensity did not change, the summer monsoon would have brought less precipitation to the East Asian land during the LGM because of the cooler SST. The decrease in SST and in evaporation then must have intensified the continental aridity, and this can be illustrated with a rough estimation of the evaporation from the South China Sea. During the LGM, shelf areas of about 1.8 million km^2 were exposed subaerially and the SST was 2–5ºC cooler than today. If the global average of sea/land difference in evaporation rate of 33.8 cm/yr (Lamb, 1972) or 50 cm/yr (Gross, 1987) is adapted, and the reduction in evaporation rate due to the SST decrease is assumed to be 10–25% (proportional to the estimates by Lamb, 1972), the decline of annual total amount of evaporation from the South China Sea at the LGM should be some 800 to 1400 $\times$ 10^9 m^3, or 1/8 to 1/4 of the annual total precipitation over whole China (P. Wang, 1995b). These rough estimations should only underline the environmental importance of the marginal seas.

4.3.2. Variability of the warm pool and 'tropical paleo-temperature enigma'

As mentioned above, the Western Pacific warm pool (Fig. 15) is responsible for a large proportion of the heat transfer from the ocean to the land and for driving the zonal Walker circulation to which the

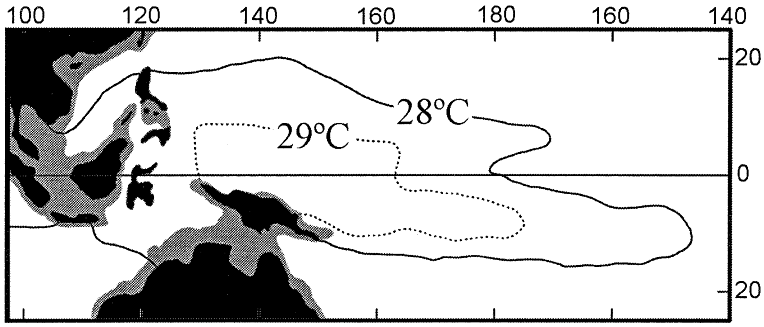

Fig. 15. Modern Western Pacific warm pool including the Sunda and Sahul shelves (shaded area denotes continental shelves emerged during the glacial maximum; isotherms taken from Yan et al., 1992).

ENSO phenomenon is closely related. Its maintenance and stability in the glacial cycles have significant implications regarding low-latitude climate conditions throughout the Indo-Pacific region (Thunell et al., 1994). However, still little is known about the response of the warm pool to the glacial cycles.

The most extensive mid- to low-latitude shelf seas, the 'Great Asian Bank' and the 'Great Australian Bank' (Fig. 12) with a total area about 3 million km^2, are developed in the Western Pacific warm pool (Fig. 15), and their emergence during glacial times reduced the size of the pool considerably. Moreover, the decrease of SST in the low-latitude marginal seas also weakens the role of the warm pool in the air–sea interactions, implying a certain instability of the pool during glacial times. The size reduction is not restricted to the marginal seas. The southern limit of the Western Pacific warm pool retreated northwards due to the northward migration of the Tasman Front in the South Pacific (Martinez, 1994) and the weakening of the Leeuwin Current in the eastern Indian Ocean (Wells and Wells, 1994), while the northern limit of the pool moved southward due to the southward shift of the Polar Front in the North Pacific (Thompson and Shackleton, 1980), leading to a reduction in latitudinal coverage of the warm pool (Martinez and De Dekker, 1996). Thus, the Western Pacific warm pool was maintained throughout the glacial times (Thunell et al., 1994), but experienced expansion and contraction and remarkable variations in its climatic role during the glacial cycles.

We are still puzzled by the paleo-temperature enigma in the glacial tropical ocean in general, and the western Pacific in particular. While very little SST changes in the glacial cycles have been found in the tropical ocean, substantial cooling during the last glacial was reported from tropical islands. In New Guinea, the alpine snow lines during the glacial times were >1000 m lower than today (Webster and Streten, 1978), and in mountains of Java and Sumatra the forest altitudinal boundaries shifted downwards during the glaciation (Stuijts et al., 1988). All these have been reconfirmed by recent studies (Van der Kaars and Dam, 1995; Peterson et al., 1996). From the discrepancy between marine and terrestrial records emerges an enigma in tropical paleoclimate studies: the glacial SST was too warm to fit the significant cooling in highlands (Rind and Peteet, 1985). Two possible solutions were proposed: either the marine or/and terrestrial paleo-temperature records have serious estimation errors, or the lapse rates during the glaciation were much steeper than today. Although the reliability of the paleo-temperature estimates has been a matter of debate, very significant errors are unlikely. As to the steeper lapse rates, this is a hypothesis still active now, but its predestinate consequence is a significant change in relative humidity in the atmosphere and, hence, a very arid climate which is not conformable to the available records, not to mention the denial of the hypothesis by the recent evidence from the noble gas content in glacial-age aquifers from North America (Anderson and Webb, 1994).

The glacial intensification of the winter monsoon may offer an alternative approach to the paleo-temperature enigma in the tropical Western Pacific. The climate variations on islands around the low-lati-

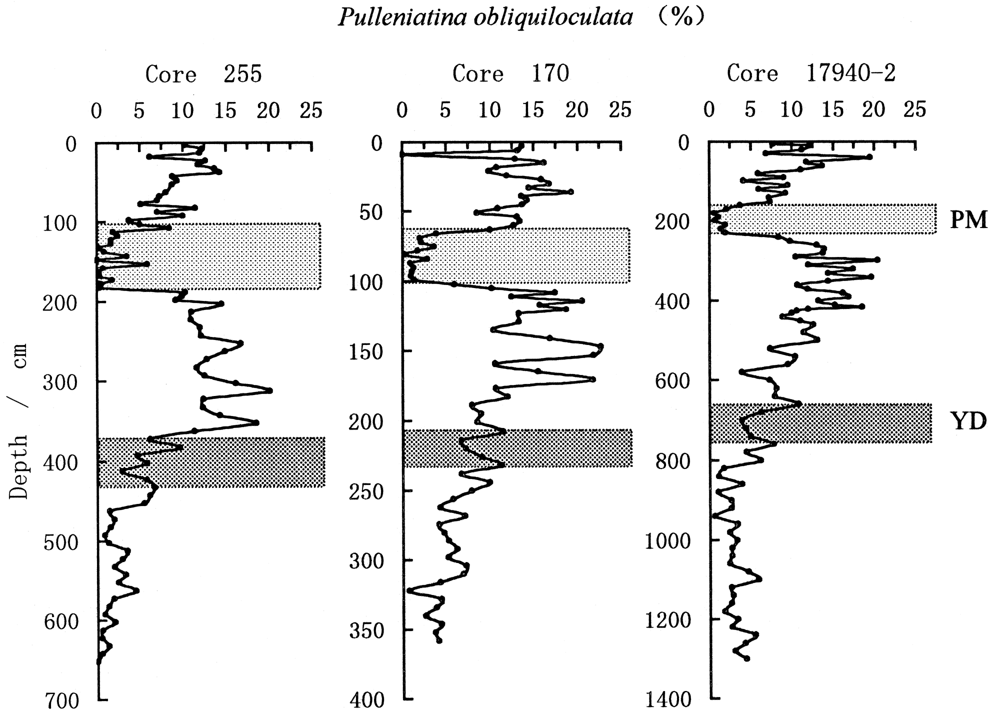

Fig. 16. Downcore variations of *Puleniatina obliquiloculata* (%) in planktonic foraminiferal fauna in cores from the East China Sea (Cores 255 and 170) and the South China Sea (Core 17940). *PM* = *Pulleniatina* minimum event; *YD* = Younger Dryas event. (Modified from Jian et al., 1996, and Li et al., 1997.)

tude marginal seas, such as Java, Sumatra and New Guinea, are under their direct influence. The modern winter monsoon transfers vapor from the marginal seas to the islands together with cold air, and the monsoon fluctuations are responsible for the variations of precipitation over the islands (Lim and Tuen, 1991). Accordingly, the intensification of the boreal winter monsoon at the LGM must have led to a combination of decreased temperature and enhanced vapor supply, what in turn might have caused the lowering of the snowline in New Guinea and the downward shift of alpine vegetation zones.

Our discussions are limited to the paleoceanographic and paleoclimatic response of the marginal seas to the glacial stage. Numerous recent publications and reports have shown great opportunities provided by high-resolution stratigraphy in marginal seas for reconstructing the history of paleoenvironmental evolution in the region. An example are the '*Pulleniatina* events' discovered in the Okinawa Trough (Core 255, 123°07′E, 25°12′N, w.d. 1575 m; Core 170, 125°48′E, 26°38′N, w.d. 1470 m) and then observed also in the South China Sea (e.g., Core 17940; Fig. 16). This tropical, deep-dwelling winter species abruptly increased in percentage about 7 ka BP and then drastically decreased about 4 ka BP ('*Pulleniatina* minimum event'), suggesting winter SST changes or Kuroshio migrations (Jian et al., 1996; Li et al., 1997). Further investigations of biological and paleoceanographic events in deep-sea sediments in marginal seas and their correlation with terrestrial records are highly promising paleoenvironmental studies.

5. Conclusions

The paleoceanographic and sedimentological response of Western Pacific marginal seas to glacial cycles depends on the extent of isolation of individual basins which can be estimated by their morphological features: ratio of sill depth to basin depth

(S/B), ratio of passage width to total surface area (P/A), and ratio of connecting section area to total basin volume (C/V). The Sea of Japan and Sulu Sea show the highest extent of isolation, followed by the South China Sea and the Sea of Okhotsk.

The sedimentation rates in the deeper parts of the marginal seas are one to two orders of magnitudes higher than in the open ocean, but in contrast to the ocean, the rates are subject to considerable variations in time and space. Down-slope sediment transport is responsible for the seaward supply of sediment to the deep sea and was most active during rapid sea-level changes, in particular during the last deglaciation, about 13 ka BP.

Four types of carbonate cycles in the late Quaternary have been recognized in the marginal seas: the 'Northwestern Pacific type' in the Sea of Okhotsk implies its connection with the NW Pacific, the 'Japan Sea type' is indicative of the isolation of the Japan Sea, the co-occurrence of the 'Atlantic type' and the 'Pacific type' in the China Seas and Sulu Sea suggests a superposition of dilution and production variations upon the dissolution cycles typical for the Pacific Ocean sediments.

Due to the absence of large icecaps in Eastern Asia, the emergence and submergence of the extensive continental shelves in the marginal seas are the most prominent geographic changes in the Western Pacific region during the glacial cycles. Three major shelves (East China Sea Shelf, Great Asian Bank, Great Australian Bank) sum to ca. 3,900,000 km^2, the latter two are located in the Western Pacific warm pool and hence have profound impact on regional climate changes.

Due to the strengthening of the winter monsoon and reorganization of sea circulation during glacial times, the winter SST was much cooler in the marginal seas than in the open ocean. As shown by the paleo-SST estimations based on the transfer function technique, the average SST in the South China Sea and Sulu Sea was 0.9ºC cooler than in the Pacific at similar latitudes in summer, while the difference was as much as 4.9ºC in winter, resulting in an enhanced seasonality in the marginal seas during the glacials. The increased glacial/interglacial SST contrast in the marginal seas has been supported by $U_{37}^{k'}$ and $\delta^{18}O$ analyses.

The glacial emergence of shallow seas and SST decrease in deeper water areas in the Western Pacific marginal seas led to a considerable reduction of evaporation. This was a major factor of the enhanced aridity in the Asian hinterland during the glacial stages. Since the low-latitude Western Pacific marginal seas are part of the Western Pacific warm pool, their emergence and cooling during the glacials must have weakened the role of the warm pool in regional climate during glacial periods. Since the strengthened winter monsoon and intensified seasonality of the marginal seas could bring cool temperature together with moisture to the islands in Southeastern Asia in the glacial, the Western Pacific marginal seas may offer an alternative approach for deciphering the 'tropical paleo-temperature enigma' in the Western Pacific.

Summarizing, the high-resolution sediment records of the Western Pacific marginal seas have a great potential for a better understanding of the variations in interactions between land and sea, as well as between individual sea basins during glacial cycles. Moreover, the sensitivity of marginal seas to sea-level changes and their close tie with the 'Western Pacific warm pool' have predestined their unusual role in regional and even global climate changes during the glacial cycles. This role, however, has up to now not yet been appropriately recognized because of two reasons: first, some of the Western Pacific marginal seas have been little studied for their modern oceanography, not to say their paleoceanography; second, the spatial resolution in global or regional paleoclimatic simulations is as a rule much too coarse for marginal seas. Therefore, much more attention is needed for research work in the region of the Western Pacific marginal seas.

Acknowledgements

This paper derives from a project supported by the National Natural Science Foundation of China (No. 49732060) and also from the WESTPASC Paleogeographic Mapping Project of the UNESCO/IOC. The manuscript greatly profitted from thorough reviews by Ulrich von Rad and Bob Thunell. Michael Sarnthein, Luejiang Wang, Zhimin Jian, Wei Huang and others are acknowledged for constructive discussions and for providing data. Wei Huang and Zhimin Jian are also thanked for their assistance in the preparation of the manuscript.

References

Ahagon, N., Tanaka, Y., Ujiie, H., 1993. *Florisphaera profunda*, a possible nannoplankton indicator of late Quaternary changes in sea-water turbidity at the northwestern margin of the Pacific. Mar. Micropaleontol. 22, 255–273.

Anderson, D., Webb, R.S., 1994. Ice-age tropics revisited. Nature 367, 23–24.

Arrhenius, G.O.S., 1952. Sediment cores from the east Pacific. Rep. Swed. Deep Sea Exped. 1947–1948, 5:1–288.

Astakhov, A.S., Gorbarenko, S.A., Tkalich, O.A., 1989. Dynamics of late Quaternary sedimentation on the continental slope of the South China Sea (in Russian). Tikhookeanskaya Geol. 4, 85–89.

Berger, W.H., 1973. Deep-sea carbonates: Pleistocene dissolution cycles. J. Foraminiferal Res. 3, 187–195.

Berger, W.H., 1992. Pacific carbonate cycles revisited: arguments for and against productivity control. In: Ishizaki, K., Saito, T. (Eds.), Centenary of Japanese Micropaleontology. Terra, Tokyo, pp. 15–25.

Berger, W.H., Killingley, J.S., Vincent, E., 1987. Time scale of the Wisconsin/Holocene transition: oxygen isotope record in the western Equatorial Pacific. Quat. Res. 28, 295–306.

Berger, W.H., Bickert, T., Schmidt, H., Wefer, G., Yasuda, M., 1993. Quaternary oxygen isotope record of pelagic foraminifers: Site 805, Ontong-Java Plateau. Proc. ODP, Sci. Results 130, 363–379.

Bian, Yunhua, Wang, Pinxian, Zheng, Lianfu, 1992. Deep-water dissolution cycles of late Quaternary planktonic foraminifera in the South China Sea (in Chinese, with English abstract). In: Ye, Z., Wang, P. (Eds.), Contributions to Late Quaternary Paleoceanography of the South China Sea. Qingdao Ocean University Press, Qingdao, pp. 261–273.

Broecker, W.S., 1991. The great ocean conveyor. Oceanography 4 (2), 79–89.

Cang, S., Yan, J., 1992. Paleoceanography of the Marginal Seas of the West Pacific (in Chinese). Qingdao Ocean University Press, Qingdao, 180 pp.

Chen, A.C.-T., Wang, S.-L., Bychkov, A.S., 1995. Carbonate chemistry of the Sea of Japan. J. Geophys. Res. 100 (C7), 13737–13745.

Chen, L., Zhu, Q., Luo, H., He, J., Dong, M., Feng, Z., 1991. The East Asian Monsoon (in Chinese). China Meteorology Press, Beijing.

Chen, M.-T., Huang, C.-Y., Wei, K.-Y., 1997. 25,000-year late Quaternary records of carbonate preservation in the South China Sea. Palaeogeogr., Palaeoclimatol., Palaeoecol. 129, 155–169.

Chinzei, K., Okada, H., Oda, M. et al., 1984. Paleoceanography since the last glacial in the Pacific along the east coast of Honshu, Japan (in Japanese). In: Scientific Research on Preservation of Cultural Properties, pp. 441–457.

CLIMAP Project Members, 1981. Seasonal reconstructions of the earth's surface at the Last Glacial Maximum. Geol. Soc. Am. Map Chart Ser. MC-36, 18 pp., 9 maps.

Dersch, M., Stein, R., 1992. Pliocene–Pleistocene fluctuations in composition and accumulation rates of peolo-marine sediments at Site 798 (Oki Ridge, Sea of Japan) and climatic change: preliminary results. Proc. ODP, Sci. Results 127/128, Pt. 1, 409–422.

Editorial Committee, Chinese Academy of Science, 1981. Physical Geography of China: Surface Water (in Chinese). Science Press, Beijing, 185 pp.

Exon, M.F., Haake, F.-W., Hartmann, M., Kogler, F.-C., Muller, P.J., Whiticar, M.J., 1981. Morphology, water characteristics and sedimentation in the silled Sulu Sea, southeast Asia. Mar. Geol. 39, 165–195.

Fairbridge, R.W. (Ed.), 1966. The Encyclopedia of Oceanography. Dowden, Hutchinson and Ross, Stroudsburg, Penn., 1021 pp.

Farrell, J.W., Prell, W.L., 1989. Climate changes and $CaCO_3$ preservation: an 800,000 year bathymetric reconstruction from the central equatorial Pacific Ocean. Paleoceanography 4, 447–466.

Feng, Wenke, Xue, W., Yang, D., 1988. The Geological Environment of Late Quaternary in the Northern South China Sea (in Chinese). Guangdong Science and Technology Publications House, Guangzhou, 261 pp.

Follmi, K.B., Cramp, A., Follmi, K.E. et al., 1992. Dark-light rhythms in the sediments of the Japan Sea: preliminary results from Site 798, with some additional results from Site 797 and 799. Proc. ODP, Sci. Rep. 127/128, Pt. 1, 559–576.

Frenzel, B., Pecsi, M., Velichko, A.A. (Eds.), 1992. Atlas of Paleoclimates and Paleoenvironments of the Northern Hemisphere. Late Pleistocene–Holocene. Geographical Research Institute, Budapest, and Gustav Fischer Verlag, Stuttgart.

Gao, L., Yan, J., Xue, S., 1992. Late Quaternary paleoceanography in the northern shelf of the South China Sea (in Chinese, with English abstract). In: Ye, Z., Wang, P. (Eds.), Contributions to the Late Quaternary Paleoceanography of the South China Sea. Qingdao Ocean University Press, Qingdao, pp. 96–107.

Gladyshev, S.V., 1993. Termohalinnyi analiz smesheniya vod v rayone Kuril'skykh Ostravov. Dokl. Akad. Nauk 331 (3), 359–363.

Gorbarenko, S.A., 1987. Paleogeography of the Japan Sea during the late Pleistocene and Holocene (in Russian). Izv. Akad. Nauk USSR, Ser. Geogr. 1987 (6), 106–113.

Gorbarenko, S.A., 1991a. Stratigraphy of late Quaternary sediments in Seas of Japan and Okhotsk and their paleoceanographic conditions. CCOP/TP 22, 11–24.

Gorbarenko, S.A., 1991b. Stratigraphy of the upper-Quaternary sediments from the central part of the Okhotsk Sea and its paleoceanography by the oxygen-isotopic method data and other methods (in Russian). Okeanologia 31 (6), 1036–1042.

Gorbarenko, S.A., 1993. The reasons for surface water mass of the Sea of Japan freshening during the latest glaciation revealed by oxygen isotopes correlation in plankton foraminifera (in Russian, with English abstract). Okeanologia 33 (3), 422–428.

Gorbarenko, S.A. et al., 1988. Late Quaternary sediments of the Okhotsk Sea and reconstruction of paleoceanographic conditions (in Russian). Pac. Ocean Geol. 198 (2), 25–34.

Gorbarenko, S.A., Pliss, S.G., Southon, J.R., et al., 1995. Detailed carbonate stratigraphy of the Japan Sea during last glaciation — Holocene. Terres. Atmos. Oceanic Sci. 6 (1), 103–113.

Gorshkov, S.G. (Ed.), 1974. Atlas Okeanov: Tikhii Okean. Voenno-Morskoi Flot SSSR 302 pp.

Gross, M.G., 1987. Oceanography: A View of the Earth. Prentice-Hall, Englewood Cliffs, N.J., 4th ed., 406 p..

Haug, G.H., Maslin, M.A., Sarnthein, M., Stax, R., Tiedmann, R., 1995. Evolution of northwest Pacific sedimentation patterns since 6 Ma (Site 882). Proc. ODP, Init. Rep. 145, 85–119.

Hay, W.W., 1994. Pleistocene–Holocene fluxes are not the Earth's norm. In: Material Fluxes on the Surface of the Earth. National Academy Press, Washington, D.C., pp. 15–26.

Huang, C.-Y., Liew, P.-M., Zhao, M., Chang, T.-C., Kuo, C.-M., Chen, M.-T., Wang, C.-H., Zheng, L., 1997a. Deep sea and lake records of the Southeast Asian paleomonsoons for the last 25 thousand years. Earth Planet. Sci. Lett. 146, 59–72.

Huang, C.-Y., Wu, S.-F., Zhao, M., Chen, M.-T. et al., 1997b. Surface ocean and monsoon climate variability in the South China Sea since the last glaciation. Mar. Micropaleontol. 32, 71–94.

Huang, W., 1997. Quantitative Study on Variations in Deepwater Sedimentation of the South China Sea during Glacial Cycles (in Chinese, with English abstract). MS Thesis, Department of Marine Geology, Tongji University, Shanghai, 65 pp.

Huang, W., Wang, P., 1998. A quantitative approach to deep-water sedimentation in the South China Sea: changes since the last glaciation. Science in China, Ser. D 41 (2), 195–201.

Hughes, B.A., Hughes, T.L., 1994. Transgressions: rethinking Beringian glaciation. Palaeogr., Palaeoclimatol., Palaeoecol. 110, 275–294.

Ikehara, K., 1992. Influence of surface water circulations on the sea bottom in the southern Japan Sea. Le Mer 30, 105–118.

Ikehara, K., Kikkawa, K., Oshima, H., 1994. Late Quaternary palaeoenvironments of the Japan Sea as revealed by tephrochronology, AMS 14-C datings and palynological data. Proc. 1994 Sapporo IGBP Symp., 14–17 Nov. 1994, Hokkaido Univ., pp. 505–510.

Jennerjahn, T.C., Liebezeit, G., Kempe, S., Xu, L.Q., Chen, W.B., Wong, H.K., 1992. Particle flux in the northern South China Sea. In: Jin, X.L. et al. (Eds.), Marine Geology and Geophysics of the South China Sea. China Ocean Press, Beijing, pp. 228–235.

Jian, Z., 1992. Sea surface temperatures in the southern continental slope of the South China Sea since last glacial and their comparison with those in the northern slope (in Chinese, with English abstract). In: Ye, Z., Wang, P. (Eds.), Contributions to Late Quaternary Paleoceanography of the South China Sea. Qingdao Ocean University, Qingdao, pp. 78–87.

Jian, Z., Li, B., Pflaumann, U., Wang, P., 1996. Late Holocene cooling event in the western Pacific. Science in China, Ser. D 39, 543–550.

Jin, X. et al., 1989. Report on study of geosciences in South China Sea (in Chinese). Donghai Mar. Sci. Hanzhou 7 (4), 1–92.

Jolivet, L., Huchon, P., Rangin, C., 1989. Tectonic setting of Western Pacific marginal basins. Tectonophysics 160, 233–247.

Jolivet, L., Tamaki, K., Fournier, M., 1994. Japan Sea, opening history and mechanism: a synthesis. J. Geophys. Res. 99 (B11), 22237–22259.

Keigwin, L.D., 1994. Northwest Pacific paleohydrography. Proc. 1994 IGBP Symp., 14–17 Nov. 1994, Hokkaido Univ., pp. 473–478.

Keigwin, L.D., Jones, G.A., Froelich, P.N., 1992. A 15,000 year paleoenvironmental record from Meiji Seamount, far northwestern Pacific. Earth Planet. Sci. Lett. 111, 425–440.

Kenyon, P.M., Turcotte, D.L., 1985. Morphology of a delta prograding by bulk sediment transport. Geol. Soc. Am. Bull. 96, 1457–1465.

Kudrass, H.R., Jin, X.L., Beiersdorf, H., Cepek, P., 1992. Erosion and sedimentation in the Xisha Trough at the continental margin of southern China. In: Jin, X.L. et al. (Eds.), Marine Geology and Geophysics of the South China Sea. China Ocean Press, Beijing, pp. 137–147.

Lamb, H.H., 1972. Climate: Present, Past and Future. Methuen, London, Vol. 1, 613 pp.

Lao, Y., Anderson, R.F., Broecker, W.S., Trumbore, S.E., Hofmann, H.J., Wolfli, W., 1992. Increased production of cosmogenic ^{10}Be during the last glacial maximum. Nature 357, 576–578.

Le, J., Shackleton, N.J., 1992. Carbonate dissolution fluctuations in the western equatorial Pacific during the late Quaternary. Paleoceanography 7, 21–42.

Li, Meng-Yang, 1995. Paleoceanography of the Northern South China Sea since the Last Glacial Maximum (in Chinese). M.S. Thesis, Taiwan Univ., 96 pp.

Li, B., Jian, Z., Wang, P., 1997. *Pulleniatina obliquiloculata* as paleoceanographic indicator in the southern Okinawa Trough since the last 20,000 years. Mar. Micropaleontol. 32, 59–69.

Li, Congxian, Chen, G., Yao, M., Wang, P., 1991. The influences of suspended load on the sedimentation in the coastal zones and continental shelves of China. Mar. Geol. 96, 341–352.

Li, Cuizhong, 1993. Micropaleontology, carbonates and oxygen isotope records in late Quaternary deep-water sediment cores of the South China Sea (in Chinese, with English abstract). Trop. Oceanogr. Guangzhou 12, 16–23.

Li, L., Tu, X., Luo, Y., Chen, S., 1992. Planktonic foraminiferal assemblages and paleoceanography of South China Sea in late Quaternary (in Chinese, with English abstract). Trop. Oceanol., Guangzhou 11 (2), 62–69.

Li, X., Chen, F., Tang, R., Fang, X., 1996. Oxygen-isotope and paleoclimate studies of Core HY4-901, northern South China Sea (in Chinese). Chin. Sci. Bull. 41 (10), 911–913.

Likht, F.R., Astakhov, A.S., Botsyl, A.I., Derkatschev, A.N. et al., 1983. Structure of Sediments and Facies of the Japan Sea

(in Russian). Academy of USSR, Far East Scientific Centre, Vladivostok, 286 pp.
Lim, J.T., Tuen, K.L., 1991. Sea surface temperature variations in the South China Sea during the Northern Hemisphere monsoon. Proc. 2nd WESTPAC Symp., December 1991, Penang, IOC, pp. 113–144.
Linsley, B.K., 1991. Carbonate sedimentation in the Sulu Sea linked to the onset of Northern Hemisphere glaciation, 2.4 Ma. Proc. ODP, Init. Rep. 124, 299–342.
Linsley, B.K., Dunbar, R.B., 1994. The late Pleistocene history of surface water $\delta^{13}C$ in the Sulu Sea: possible relationship to Pacific deepwater $\delta^{13}C$ changes. Paleoceanography 9 (2), 317–340.
Linsley, B.K., Thunell, R.C., 1990. The record of deglaciation in the Sulu Sea: evidence for the Younger Dryas event in the tropical western Pacific. Paleoceanography 5 (6), 1025–1039.
Linsley, B.K., Thunell, R.C., Morgan, C., Williams, D.F., 1985. Oxygen minimum expansion in the Sulu Sea, western equatorial Pacific, during the last glacial low stand of sea level. Mar. Micropaleontol. 9, 395–418.
Lisitzin, A.P., 1972. Sedimentation in the World Ocean. Soc. Econ. Paleontol. Mineral. Spec. Publ. 17, 218 pp.
Luz, B., Shackleton, N.J., 1975. $CaCO_3$ solution in the tropical east Pacific during the past 130,000 years. Cushman Found. Foraminiferal Res., Spec. Publ. 13, 142–150.
Lyle, M., Prahl, F., Sparrow, M., 1992. Upwelling and productivity changes inferred from a temperature record in the central equatorial Pacific. Nature 355, 812–815.
Mao, S., Harland, R., 1993. Quaternary organic-walled dinoflagellate cysts from South China Sea and their paleoclimatic significance. Palynology 17, 47–65.
Martinez, J.I., 1994. Late Pleistocene paleoceanography of the Tasman Sea: implications for the dynamics of the warm pool in the western Pacific. Palaeogeogr., Palaeoclimatol., Palaeoecol. 112, 19–62.
Martinez, J.I., De Dekker, P., 1996. The Western Pacific warm pool during the last glacial maximum (abstr.). The Environmental and Cultural History and Dynamics of the Australian–Southeast Asian Region, Program and Abstracts, Monash University.
Miao, Q., Thunell, R.C., Anderson, D.M., 1994. Glacial-Holocene carbonate dissolution and sea surface temperatures in the South China and Sulu seas. Paleoceanography 9, 269–290.
Milliman, J.D., Meade, R.H., 1983. World-wide delivery of river sediment to the ocean. J. Geol. 91 (1), 1–21.
Milliman, J.D., Syvitski, J.P.M., 1994. Geomorphic/tectonic control of sediment discharge to the ocean: the importance of small mountainous rivers. In: Material Fluxes on the Surface of the Earth. National Academy Press, Washington, D.C., pp. 74–85.
Min, Q., Zhao, Q., Wang, P., 1992. Paleoceanography of the outer shelf, northern South China Sea: a preliminary study. In: Ye, Z., Wang, P. (Eds.), Contributions to Late Quaternary Paleoceanography of the South China Sea (in Chinese, with English abstract). Qingdao Ocean University, Qingdao, pp. 108–118.
MOET (The Multidisciplinary Oceanographic Expedition Team of Chinese Academy of Science to the Nansha Islands), 1993. Quaternary Sedimentary Geology of Nansha Islands and Adjacent Sea Area (in Chinese). Hubei Sci. Technol. Press, 383 pp.
Moore Jr., T.C., Burckle, L.H., Geitzenauer, K. et al., 1980. The reconstruction of sea surface temperatures in the Pacific Ocean of 18,000 B.P. Mar. Micropaleontol. 5, 215–247.
Morton, R.A., 1993. Attributes and origins of ancient submarine slides and filled embayments: examples from the Gulf Coast Basin. Am. Assoc. Pet. Geol. Bull. 77, 1064–1081.
Nittrouer, C.A., Wright, L.D., 1994. Transport of particles across continental shelves. Rev. Geophys. 32, 85–113.
Oba, T., 1982. Paleoenvironments of the Sea of Japan since the last glaciation (in Japanese). Chikyu 5 (1), 37–46.
Oba, T., Niitsuma, N., Saito, T., 1983. Isotope stratigraphy of the upper Quaternary in the seas around Japan. Kaiyo Kagaku (Mar. Sci.) 15, 130–137.
Oba, T., Kato, M., Kitazato, H., Koizumi, I., Omura, A., Sakai, T., Takayama, T., 1991. Paleoenvironmental changes in the Japan Sea during the last 85,000 years. Paleoceanography 6, 499–518.
Pelejero, C., Grimalt, J.O., Sarnthein, M., Wang, L., 1996. Variations in $U_{37}^{k'}$ surface temperature and marine/terrestrial biomarkers in the South China Sea during the last 130,000 years (abstr.). IGC-30, Abstr. Vol. 2, p. 253.
Peterson, J., Hope, G., Hantoro, W. et al., 1996. Irian Java glaciers and late Quaternary tropical temperature estimates (abstr.). Int. Symp. Environmental and Cultural History and Dynamics of the Australian–Southeast Asian Region, Monash University, December 1996, Programme and Abstracts.
Pflaumann, U., Jian, Z., 1999. Modern distribution patterns of planktonic foraminifera in the South China Sea and West Pacific: a new transfer technique to estimate regional sea-surface temperatures. Mar. Geol. 156, 41–83.
Qin, Yunshan, Li, F., Tang, B., Milliman, J.D., 1986. Buried paleoriver system in western part of the South Huang Sea (in Chinese). Kexue Tongbao, 31: 1887–1889.
Quadfasel, D., Kudrass, H., Frische, A., 1990. Deep-water renewal by turbidity currents in the Sulu Sea. Nature 348, 320–322.
Rind, D., Peteet, D., 1985. Terrestrial conditions at the last glacial maximum and CLIMAP sea-surface temperature estimations: are they consistent? Quat. Res. 24, 1–22.
Ross, W.C., Halliwell, B.A., May, J.A., Watts, D.E., Syvitsky, J.P.M., 1994. Slope readjustment: a new model for the development of submarine fan and aprons. Geology 22, 511–514.
Rottmen, M.L., 1979. Dissolution of planktonic foraminifera and pteropods in South China Sea sediments. J. Foraminiferal Res. 9, 41–49.
Rutter, N., 1995. Problematic ice sheets. Quat. Int. 28, 19–37.
Sarnthein, M., Pflaumann, U., Wang, P.X., Wong, H.K. (Eds.), 1994. Preliminary Report on Sonne-95 Cruise ‘Monitor Monsoon’ to the South China Sea. Rep., Geol. Paläontol. Inst. Univ. Kiel 68, 1–125.
Schönfeld, J., Kudrass, H.-R., 1993. Hemipelagic sediment accu-

mulation rates in the South China Sea related to late Quaternary sea-level changes. Quat. Res. 40, 368–379.
Seibold, E., 1970. Nebenmeere im humiden und ariden Klimabereich. Geol. Rundsch. 60, 73–105.
Seibold, E., Berger, W.H., 1993. The Sea Floor: An Introduction to Marine Geology. Springer-Verlag, Berlin.
Sher, A., 1995. Is there any real evidence for a huge shelf ice sheet in East Siberia? Quat. Int. 28, 39–40.
Stuijts, I., Newsome, J., Flenly, J., 1988. Evidence for late Quaternary vegetational change in the Sumatran and Javan highlands. Rev. Paleobot. Palynol. 55, 207–216.
Sudo, H., 1986. A note on the Japan Sea Proper Water. Progr. Oceanogr. 17, 313–336.
Sun, Xiangjun, Li, Xun, 1999. A pollen record of the last 37 ka in deep sea core 17940 from the northern slope of the South China Sea. Mar. Geol. 156, 227–242.
Tada, R., Koizumi, I., Cramp, A., Rahman, A., 1992. Correlation of dark and light layers, and the origin of their cyclicity in the Quaternary sediments from the Japan Sea. Proc. ODP, Sci. Rep. Pt. 1 127/128, 577–601.
Talley, L.D., 1996. North Pacific Intermediate Water formation and the role of the Okhotsk Sea. Proc. Workshop Okhotsk Sea and Adjacent Areas, Sept. 1996, PICES Sci. Rep. 6, pp. 150–157.
Talley, L.D., Nagata, Y. (Eds.), 1995. The Okhotsk Sea and Oyashio Region. PICES Sci. Rep. 2, 226 pp.
Tamaki, K., Honza, E., 1991. Global tectonics and formation of marginal basins: role of the western Pacific. Episodes 14, 224–2230.
Taylor, B., Natland, J. (Eds.), 1995. Active Margins and Marginal Basins of the Western Pacific. Am. Geophys. Union, Geophys. Monogr. 88, 1–417.
Thompson, P.R., 1981. Planktonic Foraminifera in the western North Pacific during the past 150,000 years: comparison of modern and fossil assemblages. Palaeogeogr., Palaeoclimatol., Palaeoecol. 35, 241–279.
Thompson, P.R., Shackleton, N.J., 1980. North Pacific palaeoceanography: late Quaternary coiling variations of planktonic foraminifer *Neogloboquadrina pachyderma*. Nature 287, 829–833.
Thunell, R., Miao, Q., Calvert, S.E., Pedersen, T.F., 1992. Glacial-Holocene biogenic sedimentation patterns in the South China Sea: productivity variations and surface p_{CO_2}. Paleoceanography 7, 143–162.
Thunell, R., Anderson, D., Gellar, D., Miao, Q., 1994. Sea-surface temperature estimates for the tropical Western Pacific during the last glaciation and their implications for the Pacific Warm Pool. Quat. Res. 41, 255–264.
Torgersen, T., Hutchinson, M.F., Searle, D.E., Nix, H.A., 1983. General bathymetry of the Gulf of Carpentaria and the Quaternary physiography of Lake Carpentaria. Palaeogeogr., Palaeoclimatol., Palaeoecol. 41, 207–225.
Umgrove, J.H.F., 1949. Structural History of the East Indies. Cambridge University Press, Cambridge.
UNESCO/IOC, 1995. WESTPAC Paleogeographic Maps. The Last Glacial Maximum Paleogeographic Map for the Western Pacific Region. Tongji University, Shanghai.
Van der Kaars, W.A., Dam, M.A.C., 1995. A 135,000 years record of vegetational and climatic changes from the Bandung area, West-Java, Indonesia. Palaeogeogr., Palaeoclimatol., Palaeoecol. 117, 55–72.
Vollbrecht, R., Kudrass, H.R., 1990. Geological results of a pre-site survey for ODP drill sites in the Sulu Basin. Proc. ODP, Init. Rep. 124, 105–111.
Wang, C.-H., Chen, M.P., 1990. Upper Pleistocene oxygen and carbon isotopic changes of Core SCS-15B at the South China Sea. J. Southeast Asian Earth Sci. 4 (3), 243–246.
Wang, C.-H., Chen, M.P., Lo, S.C., Wu, J.C., 1986. Stable isotope records of late Pleistocene sediments from the South China Sea. Bull. Inst. Earth Sci., Acad. Sin. Taipei 6, 185–195.
Wang, H., 1992. Sedimentological indicators of deep sea currents to the southwest of Zhongsha Islands, South China Sea (in Chinese, with English abstract). In: Ye, Z., Wang, P. (Eds.), Contributions to Late Quaternary Paleoceanography of the South China Sea. Qingdao Ocean University Press, Qingdao, pp. 206–218.
Wang, H., Jian, Z., 1992. Carbonate dilution cycles in the late Quaternary South China Sea (in Chinese, with English abstract). In: Ye, Z., Wang, P. (Eds.), Contributions to Late Quaternary Paleoceanography of the South China Sea. Qingdao Ocean University Press, Qingdao, pp. 283–294.
Wang, L., Wang, P., 1990. Late Quaternary paleoceanography of the South China Sea: interglacial contrasts in an enclosed basin. Paleoceanography 5 (1), 77–90.
Wang, L., Pflaumann, U., Sarnthein, M., 1995. High-resolution sediment records of climatic change in the South China Sea during the past 30,000 years (abstract). ICP V Program and Abstracts, Halifax, pp. 175–176.
Wang, L., Jian, Z., Chen, J., 1997. Late Quaternary pteropods in the South China Sea: carbonate preservation and paleoenvironmental variation. Mar. Micropaleontol. 32, 115–126.
Wang, L., Sarnthein, M., Erlenkeuser, H., Grimalt, J., Grootes, P. et al., 1999. East Asian monsoon climate during the Late Pleistocene: high-resolution sediment records from the South China Sea. Mar. Geol. 156, 245–284.
Wang, P., 1990. The ice-age China Sea — research results and problems. In: Wang, P. et al. (Eds.), Proceedings of the First International Conference on Asian Marine Geology. China Ocean Press, pp. 181–197.
Wang, P., 1991. West Pacific marginal seas in last glaciation: paleogeography and its environmental impact. Proc. 2nd WESTPAC Symp. 2–6 December 1991, Penang, pp. 33–48.
Wang, P., 1995a. West Pacific marginal seas and monsoon climate change in last glacial maximum (abstract). ICP V Program and Abstracts, Halifax, p. 207.
Wang, P., 1995b. The role of West Pacific marginal seas in glacial aridification of China: a preliminary study (in Chinese, with English abstract). Quat. Sci., Beijing 1995, 32–42.
Wang, P., 1996. Response of West Pacific marginal seas to glacial cycles: paleoceanographic and sedimentological features (abstract) . 30th Int. Geol. Congr., Abstr. 3, 585.
Wang, P., 1998. Northwestern Pacific marginal seas as a hydrological system in global climate changes (in prep.).

Wang, P., Min, Q., Bian, Y., Feng, W., 1986. Planktonic foraminifera in the continental slope of the northern South China Sea during the last 130,000 years and their paleoceanographic implications. Acta Geol. Sin. (Trial English Edition) 60, 1–11.

Wang, P., Wang, L., Bian, Y., Jian, Z., 1995. Late Quaternary paleoceanography of the South China Sea: surface circulation and carbonate cycles. Mar. Geol. 127, 145–165.

Wang, P., Bradshaw, M., Ganzei, S.S., Tsukawaki, S., Hassan, K.B., Hantoro, W.S., Poobrasert, S., Burne, R., Zhao, Q., Kagami, H., 1997. West Pacific marginal seas during last glacial maximum: amplification of environmental signals and its impact on monsoon climate. Proc., 30th Int. Geol. Congr., Vol. 13, pp. 65–86.

Webster, P.J., Streten, N.A., 1978. Late Quaternary ice age climates of tropical Australasia: interpretations and reconstructions. Quat. Res. 10, 279–309.

Wells, P.E., Wells, G.M., 1994. Large-scale reorganization of ocean currents off shore western Australia during the late Quaternary. Mar. Micropaleontol. 24, 1567–1586.

Winn, K., Zheng, L., Erlenkeuser, H., Stoffers, P., 1992. Oxygen/carbon isotopes and paleoproductivity in the South China Sea during the past 110,000 years. In: Jing, X. et al. (Eds.), Marine Geology and Geophysics of the South China Sea. China Ocean Press, Beijing, pp. 154–166.

Wu, G., Yasuda, M.K., Berger, W.H., 1991. Late Pleistocene carbonate stratigraphy on Ontong-Java Plateau: effects of winnowing and dissolution. Mar. Geol. 96, 193–209.

Xu, X., Oda, M., 1995. Surface water changes in the Ryukyu Trench slope region, western margin of the North Pacific during the last 320,000 years. Trans. Proc. Paleontol. Soc. Jpn., N.S. 178, 105–121.

Yan, J., 1989. Carbonate cycles in sediments of the Western Pacific marginal seas (in Chinese). Mar. Sci., Qingdao 5, 28–32.

Yan, X., Ho, C., Zheng, Q. et al., 1992. Temperature and size variabilities of the Western Pacific Warm Pool. Science 258, 1643–1645.

Zheng, L., Ke, J., Winn, K., Stoffers, P., 1993. Carbonate sedimentation cycles in the northern South China Sea during the late Quaternary (in Chinese, with English abstract). In: Zheng, L., Chen, W. (Eds.), Contributions to Sedimentation Process and Geochemistry of the South China Sea. China Ocean Press, Beijing, pp. 109–123.

Zhou, B., Zhao, Q., 1999. Allochthonous ostracods in South China Sea and their significance in indicating sediment downslope contamination. Mar. Geol. 156, 187–195.